

# Energy & Environmental Science

Accepted Manuscript



This is an Accepted Manuscript, which has been through the Royal Society of Chemistry peer review process and has been accepted for publication.

Accepted Manuscripts are published online shortly after acceptance, before technical editing, formatting and proof reading. Using this free service, authors can make their results available to the community, in citable form, before we publish the edited article. We will replace this Accepted Manuscript with the edited and formatted Advance Article as soon as it is available.

You can find more information about Accepted Manuscripts in the [Information for Authors](#).

Please note that technical editing may introduce minor changes to the text and/or graphics, which may alter content. The journal's standard [Terms & Conditions](#) and the [Ethical guidelines](#) still apply. In no event shall the Royal Society of Chemistry be held responsible for any errors or omissions in this Accepted Manuscript or any consequences arising from the use of any information it contains.

# Design and construction of three dimensional graphene-based composites for lithium ion battery applications

Bin Luo, Linjie Zhi\*

<sup>5</sup> DOI: 10.1039/b000000x [DO NOT ALTER/DELETE THIS TEXT]

Three dimensional graphene-based composites (3DGCs) have attracted great attention for lithium ion battery applications due to their unique structures and attractive properties. A large number of 3DGCs with novel structures and functions have been developed in the past few years. This <sup>10</sup> review summarizes the current progress of 3DGCs, including their preparation and application in lithium ion batteries, especially from the viewpoint of structural and interfacial engineering, which have attracted more and more attention for the development of high performance electrode systems.

## <sup>15</sup> 1 Introduction

Over the past decade, graphene, a single atomic layer of graphite, has generated enormous excitement because of its extraordinary physical and chemical properties, including excellent electronic conductivity, superior mechanical properties, and huge theoretical specific surface area.<sup>1-10</sup> As a wonderful 2D building block, <sup>20</sup> graphene not only can be assembled into various functional macroscopic structures, e.g. graphene fibres, films, papers and sponges,<sup>11, 12</sup> but its application can be extremely extended by further functionalized or hybridized with other components, providing advanced functions with improved performance.<sup>8, 13, 14</sup> In particular, due to their excellent electrical conductivity, adjustable porosity and unique mechanical <sup>25</sup> characteristics, three dimensional graphene-based composites (3DGCs) have been attracting increasing attention in many fields such as energy storage, catalysis, sensors, electronics, and so on.<sup>15-22</sup>

New energy technologies are critically important for realizing an energy requirement that is compatible with the goal of sustainable human being development. For this <sup>30</sup> purpose, lithium-ion batteries (LIBs) are becoming more and more attractive for the ever-enlarging markets of portable electronic products, communication facilities, and electric vehicles.<sup>23</sup> Huge demand has motivated scientific and technological efforts dedicated to developing LIBs with superior performances, such as higher energy density, higher power density, and longer cycle life. To achieve these characters, the structure, <sup>35</sup> morphology, composition, ionic diffusion kinetics, electrical conductivity, as well as surface characteristics of the electrode materials need to be systematically addressed.<sup>24-27</sup> Due to the unique physicochemical properties, rationally designed 3DGCs have emerged as promising candidates for the electrode materials in lithium ion batteries.<sup>16, 28-33</sup> Introducing another functional substance into the composite can not only act as a <sup>40</sup> substantial physical barrier to separate graphene nanosheets with each other, but also function to endow the resulting composites with significantly enhanced lithium storage capability. In the mean time, owing to the existence of a synergistic effect, the separated graphene nanosheets can be a robust conductive and flexible matrix to

electrically bind the introduced components together, thus maintaining the integrity of 3DGCs electrode materials upon cycling.

In this context, considerable efforts have been devoted to the development of graphene-based composites for LIB applications. A number of synthetic strategies for 3DGCs have been developed based on the methods of either *in situ* growth or *ex situ* assembly as schematically illustrated in **Fig. 1**. Meanwhile, various nanostructured metallic, metalloid materials and metal compounds with different dimensionalities, such as zero-dimensional (0D) nanoparticles (NPs), one-dimensional (1D) nanowires and/or nanotubes, and two-dimensional (2D) nanoplates and nanosheets, have been developed and integrated onto graphene to construct graphene-based composite units. These units are then used as building blocks to fabricate functional materials/architectures with ordered or disordered alignments. A series of reviews have been published focusing on the fabrication, properties, and/or application of graphene and graphene-based nanomaterials,<sup>10, 11, 13, 15-22, 28, 31, 34-44</sup> particularly, the progress made in graphene-based composites has been scattered in several reviews either with a focus on preparation methods, or on specific applications in energy or environmental issues.<sup>13, 15, 18, 21, 28, 36, 39, 43, 45</sup> However, a whole view of the preparation-structure-performance relationship of the 3DGCs for LIBs application is still missing. In this review, we will summarize the recent advances in developing 3DGCs from the structural point of view, and highlights the importance of dimensions and interfaces in the rational design and construction of these composite materials. This review is specifically targeted to provide new perspectives on the combination of graphene and electrochemically active substances, which plays a rather important role in developing advanced electrode systems for next generation LIBs. The challenges and perspective of these emerging composites are discussed as well.

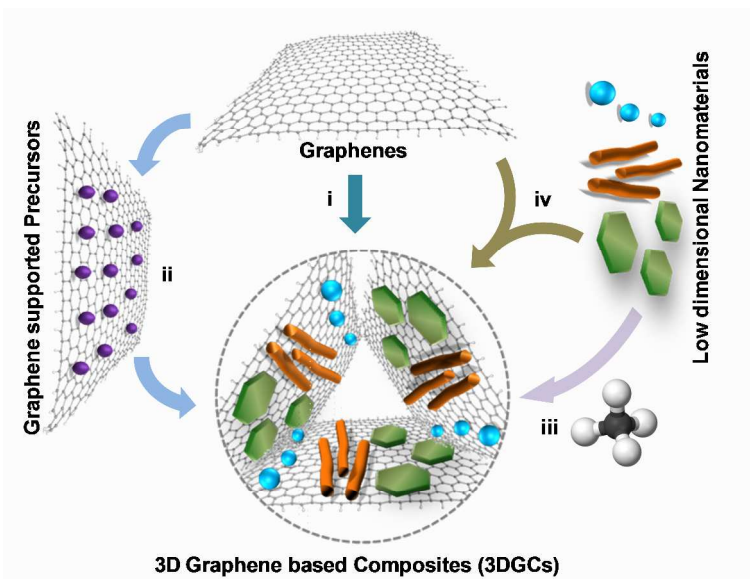


**Fig. 1** Schematic illustration of synthetic methods of 3D graphene-based composites.

## 2 Synthesis of 3D graphene-based composites

In the past few years, tremendous efforts have been devoted to the development of synthetic methods for preparing 3DGCs with various morphologies, structures and properties. As illustrated in Fig. 1, the presently reported synthetic methods of 3DGCs could be roughly divided into four categories: i) one-step *in situ* growth of nanomaterials on graphenes, ii) multi-step *in situ* conversion of nanomaterials on graphenes, iii) *ex situ* assembly of graphenes and other nanomaterials, and iv) *in situ* growth of graphenes on low dimensional nanomaterials. The term “graphenes” in this review refers to graphene, graphene derivates (e.g. graphene oxide(GO), reduced graphene oxide (RGO)), and graphene based macroscopic structures (e.g. graphene films, papers or sponges). The following subsections will discuss in detail these methods and the produced composite materials.

### 2.1 One-step *in situ* growth of nanomaterials on graphenes

Among the four approaches, one-step *in situ* growth of nanomaterials on graphenes is widely used in the synthesis of 3DGCs. This *in situ* approach mainly involves the direct formation of nanocrystallites in the present of graphenes and then the nanocrystallites directly grow into low dimensional nanomaterials, including nanoparticles<sup>46-54</sup>, nanowires<sup>55</sup>, nanorods<sup>56, 57</sup> and nanoplates<sup>58-60</sup>, on the surface of the graphenes. One advantage of this route is to avoid using protecting surfactant or extra linker molecules which may imply a tedious experimental procedure and influence the functions of the nanocomposites as well.

A variety of chemical and physical synthesis techniques, including hydrothermal/solvothermal techniques<sup>51, 61-74</sup>, gas-phase deposition<sup>55, 75-78</sup>, sol-gel processing<sup>79</sup>, and so on, have been used in the *in situ* approach. Among them, hydrothermal and solvothermal syntheses have been frequently selected in making 3DGCs with various anodic or cathodic electrochemically active nanomaterials. The one-pot process can obtain nanostructures with high crystallinity without post-synthetic annealing or calcination. Typically, SnO<sub>2</sub> nanorods were *in situ* grown on graphene sheets via a one-step hydrothermal procedure.<sup>57</sup> The obtained graphene/SnO<sub>2</sub> composites with individual SnO<sub>2</sub> nanorods of 10-20 nm in diameter and 100-200 nm in length showed a high reversible specific capacity and outstanding cycling stability as anode materials for LIBs. In another case, Chen *et al.* reported the synthesis of a novel hollow porous Fe<sub>3</sub>O<sub>4</sub>/RGO composite structure via a facile solvothermal route.<sup>69</sup> The formation of hollow porous Fe<sub>3</sub>O<sub>4</sub> beads and reduction of GO into RGO were accomplished in one step by using ethylene glycol as a reducing agent. Very recently, Yang *et al.* fabricated VO<sub>2</sub>-graphene ribbons by a simultaneous hydrothermal synthesis and reduction of layered V<sub>2</sub>O<sub>5</sub>-graphite oxide composites (**Fig. 2**). GO was used as the substrate for the *in situ* growth of VO<sub>2</sub> ribbons via the reduction of V<sub>2</sub>O<sub>5</sub> by GO. The resulting ribbons and residual graphene oxide sheets simultaneously became building blocks for the construction of 3D interpenetrating architectures.

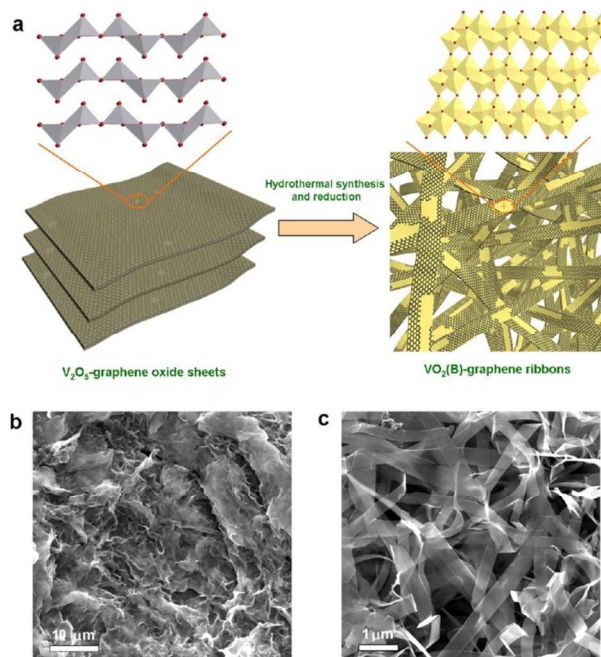


**Fig. 2** Synthesis of VO<sub>2</sub>-graphene ribbons. (a) Fabrication of VO<sub>2</sub>-graphene ribbons by a simultaneous hydrothermal synthesis and reduction of layered V<sub>2</sub>O<sub>5</sub>-graphite oxide composites at 180 °C. Typical FE-SEM images of (b) V<sub>2</sub>O<sub>5</sub>-graphite oxide composites and (c) VO<sub>2</sub>-graphene sample hydrothermally treated for 1.5 and 12 h. Reproduced with permission from ref.<sup>70</sup>. Copyright 2013, American Chemical Society.

## 2.2 Multi-step *in situ* conversion of nanomaterials on graphenes

Unlike the one-step *in situ* growth methods, the multi-step *in situ* conversion approaches always involve preloading of various precursors onto the surface of graphenes followed with a chemical conversion process to obtain the targeting nanostructures. A series of electrochemically active nanomaterials including Fe<sub>2</sub>O<sub>3</sub><sup>80</sup>, Fe<sub>3</sub>O<sub>4</sub><sup>81-83</sup>, Co<sub>3</sub>O<sub>4</sub><sup>84, 85</sup>, TiO<sub>2</sub><sup>86</sup>, Sn<sup>87-89</sup>, SnS<sub>2</sub><sup>90</sup>, Si<sup>91</sup>, V<sub>2</sub>O<sub>5</sub>,<sup>92</sup> VN,<sup>93</sup> LiMn<sub>1-x</sub>Fe<sub>x</sub>PO<sub>4</sub><sup>94</sup>, Li<sub>4</sub>Ti<sub>5</sub>O<sub>12</sub><sup>95</sup> and so on, have been prepared on graphenes in this way. So far, thermal decomposition of pre-loaded hydroxide on graphenes is a powerful strategy for preparing 3DGCs.<sup>82, 96, 97</sup> For example, RGO-wrapped Fe<sub>3</sub>O<sub>4</sub> composites (RGO/Fe<sub>3</sub>O<sub>4</sub>) have been prepared using a two-step *in situ* conversion process.<sup>82</sup> Spindle-shaped FeOOH was firstly formed on RGO by hydrolysing iron chloride hexahydrate and then converted into Fe<sub>3</sub>O<sub>4</sub> via a post-annealing process. Recently, decomposition of other precursors (e.g. metal complexes) has also been used to prepare 3DGCs.<sup>81, 98</sup>

Besides the changes in composition, dimensional conversion can also be realized through rationally designed multi-step approach, which provides a new way to construct more complex nanoarchitectures. Our recent works have demonstrated that pre-loaded metal oxide nanoparticles on the surface of graphenes can be *in situ* converted into 2D metal or metal disulfide nanosheets or 1D carbon encapsulated metal nanocables.<sup>88-90</sup> For example, a facile approach towards the synthesis of

graphene-SnS<sub>2</sub> 2D/2D composites (**Fig. 3**) has been developed by transforming SnO<sub>2</sub> nanoparticles into 2D SnS<sub>2</sub> nanoplates directly on/between graphene nanosheets via a chemical solution method followed by a simple CVD process (Figure 7a, b).<sup>90</sup> It is expected to extend the available method for the growth and assembly of various inorganic-graphene composites, which definitely encourages extensive applications in other areas. Additionally, a two-step conversion approach for the synthesis of olivine-type lithium transition-metal phosphates (LiMn<sub>1-x</sub>Fe<sub>x</sub>PO<sub>4</sub>) nanorods on RGO sheets has been reported recently.<sup>94</sup> Fe-doped Mn<sub>3</sub>O<sub>4</sub> nanoparticles were first selectively grown onto GO by controlled hydrolysis. The oxide nanoparticle precursors then reacted solvothermally with Li and phosphate ions and were transformed into LiMn<sub>1-x</sub>Fe<sub>x</sub>PO<sub>4</sub> on the surface of RGO sheets.

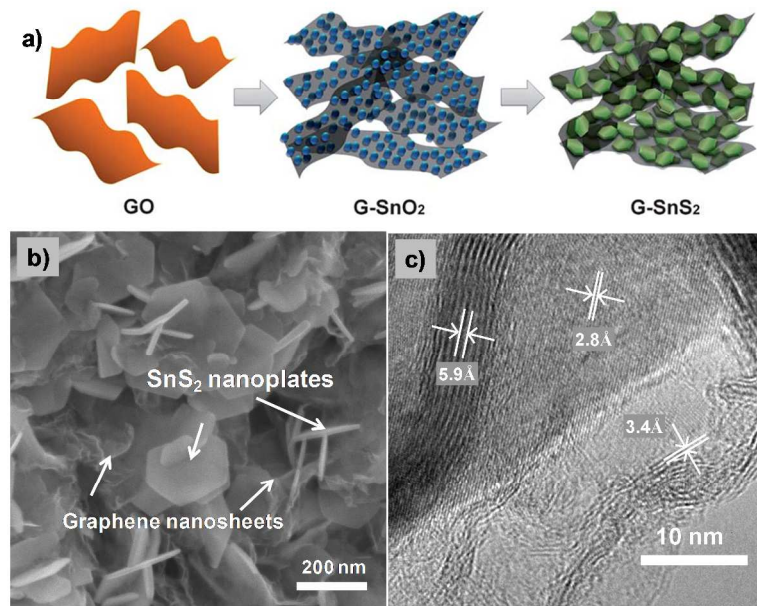


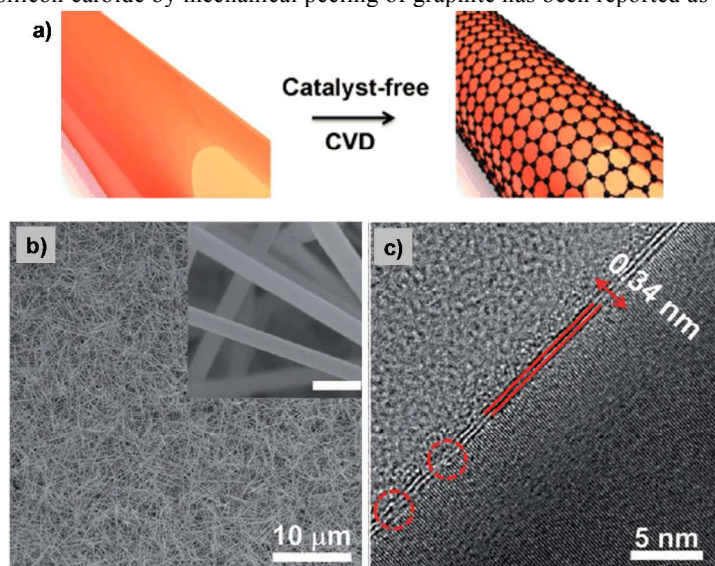
**Fig. 3** (a) Illustration of the formation of the G-SnS<sub>2</sub> involving two steps: 1) tin oxide nanoparticles were firstly decorated on graphene nanosheets and 2) converted into metal disulfide nanoplates via a solid-gas reaction. Typical (b) SEM and (c) TEM images of the G-SnS<sub>2</sub>, showing its 3D porous structure composed of two kinds of 2D nanomaterials. Reproduced from ref. <sup>90</sup> with permission from the Royal Society of Chemistry.

### 2.3 *In situ* growth of graphenes on nanomaterials

This *in situ* approach is applicable to the occasions that the active nanomaterials have been synthesized in advance. An ideal strategy to protect these active nanostructures is via *in situ* graphene encapsulation on their surface, which would provide not only the mechanical tight holding of the active nanostructures, but also high electrical conductivity across the electrode. Recently, Kim *et al.* reported the direct growth of few-layer graphene on the surface of Ge nanowires (**Fig. 4**).<sup>99</sup> The number of layers of the *in situ* grown graphene ranges from a single up to four layers, and the quality of graphene in terms of the defect level is comparable to that of

graphene grown by a conventional metal-catalyzed CVD process. Soon afterwards, Wang *et al.* reported another route to prepare highly crystalline *in situ* graphene encapsulated Ge nanowires (Ge@G) via an arc-discharge method.<sup>100</sup> The Ge nanowires are well encapsulated by few-layer graphene and are located in a network composed of graphene sheets.

There also have been reports on other active nanostructures encapsulated by a graphitic carbon layer produced with CVD methods. For example, several types of carbon encapsulated 1D Si nanostructures, including overlapped graphene sheath encapsulated Si nanowires<sup>101</sup>, graphitic carbon wrapped Si nanowires<sup>102</sup> and porous Si nanowire arrays<sup>103</sup>, have been developed recently through *in situ* growth of graphitic carbon layer on Si nanostructures. In addition to the CVD grown graphenes from a bottom-up view, another *in situ* approach to prepare few-layer graphene coated tin oxide-silicon carbide by mechanical peeling of graphite has been reported as well.<sup>104</sup>



<sup>15</sup> **Fig. 4** (a) Illustration of the formation of the graphene layer on Ge nanowire via a catalyst-free CVD process. Typical (b) SEM and (c) TEM images of the Ge@graphene composite. Reproduced with permission from ref. <sup>99</sup>. Copyright 2013, WILEY-VCH Verlag GmbH & Co. KgaA.

#### 2.4 *Ex situ* assembly of graphenes and other nanomaterials

<sup>20</sup> *Ex situ* assembly approaches mainly involve the prior synthesis of nanomaterials in the desired dimensions and morphology, then modified and subsequently connected to the surface of graphenes via covalent or non covalent interactions.<sup>18</sup> In this approach, either graphenes or the second component (or both) require modification with functional groups. Compared to *in situ* growth approaches, this self-assembly based method benefits for overcoming any incompatibility between nanomaterials synthesis and the formation of nanocomposites. Normally, GO rather than RGO is preferred to be used to anchor inorganic components due to its large amount of oxygen containing groups, facilitating the linkage with other functional groups via covalent interactions.<sup>105, 106</sup> 3D graphene/Fe<sub>3</sub>O<sub>4</sub> composites have been prepared via <sup>25</sup> an self-assembly of graphene obtained by a mild chemical reduction of GO in water

in the presence of  $\text{Fe}_3\text{O}_4$  nanoparticles.<sup>107</sup> During the formation of the 3D architecture, apart from being captured by the physical entrapment, the  $\text{Fe}_3\text{O}_4$  nanoparticles could be fixed homogeneously on both sides of GO by the formation of new bonds (such as -COO-) between  $\text{Fe}_3\text{O}_4$  and GO due to the abundant -COOH and -OH groups on GO, and those nanoparticles were retained onto the surface of graphene sheets by chemical attachment after GO was reduced.

Other non covalent interactions, such as electrostatic interactions<sup>108, 109</sup>, have also been utilized to prepare 3DGCs. GO/RGO are negatively charged with oxygen-containing functional groups on them, which can be used to assemble with positively charged inorganic NPs through electrostatic interactions. For instance, a novel strategy for the fabrication of RGO-encapsulated oxide (silica,  $\text{Co}_3\text{O}_4$ ) NPs was developed by coassembly between negatively charged GO and positively charged oxide NPs (**Fig. 5**).  $\text{SiO}_2$  or  $\text{Co}_3\text{O}_4$  NPs are firstly positively charged by aminopropyltrimethoxysilane (APS) modification and then encapsulated with negatively charged GO sheets through electrostatic interaction; the GO can be *in situ* reduced to RGO subsequently without destroying the sheet-encapsulated-particle structures.<sup>109</sup>

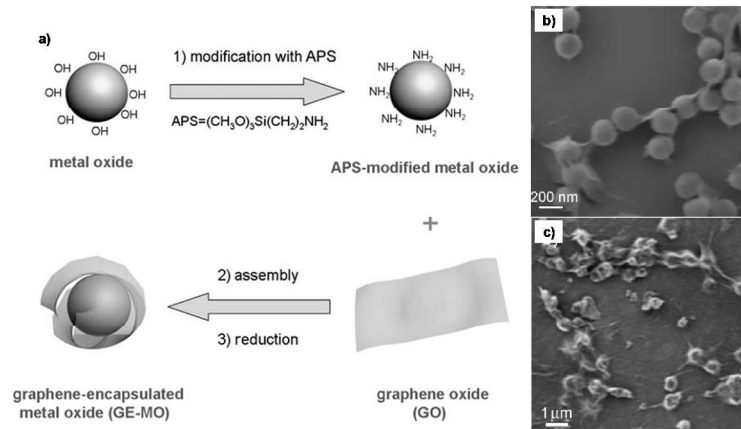


**Fig. 5** (a) Fabrication of graphene-encapsulated metal oxide (GE-MO) including 1) modification of the metal oxide by grafting aminopropyltrimethoxysilane (APS) to render the oxide surface positively charged; 2) hybrid assembly between positively charged oxide nanoparticles and negatively charged graphene oxide by electrostatic interactions; and 3) chemical reduction. Typical SEM images of (b) graphene-encapsulated silica spheres and (c) graphene-encapsulated  $\text{Co}_3\text{O}_4$ . Reproduced with permission from ref.<sup>109</sup>. Copyright 2010, WILEY-VCH Verlag GmbH & Co. KgaA.

### 3 Structural and interfacial engineering of 3DGCs for LIBs

It is well known that the composition and morphology of the active material, as well as its interfacial contacts with current collector and electrolyte, have great influence on the electrochemical performances of the electrode.<sup>110, 111</sup> In this section, we will summarize the progress of 3DGCs for LIBs from a point of view of structural and interfacial engineering, including the structural design of electrochemically active nanomaterials, the graphene layer orientation within the composite, the interfacial contact between graphene and active nanomaterials and the interfacial contact of the composite with the electrolyte.

### 3.1 Structural design of electrochemically active nanomaterials

Nanostructured active materials have been demonstrated with enhanced Li-ion storage capability by increasing the specific surface area for interfacial reactions and the flux of Li-ions across the electrode-electrolyte interface.<sup>112-116</sup> Recently, the development and implementation of graphene-based composites with other low dimensional nanomaterials (e.g. 0D nanoparticles, 1D nanowires, 2D nanosheets) has led to great enhancements in LIB performance.

Among electrochemically active nanomaterials with different dimensionalities, 0D nanoparticles are the most likely ones to be applied in commercialized batteries,<sup>10</sup> mainly due to their scalable production possibilities. Attaching 0D nanoparticles onto 2D graphene nanosheets is an efficient strategy to enable the formation of highly efficient conductive network, alleviate the aggregation of 0D nanoparticles, and accommodate as well the volume expansion of the inorganic substances during the charge-discharge process. Taking SnO<sub>2</sub>-based anodes as an example, Paek *et al.*<sup>15</sup> have recently attached SnO<sub>2</sub> nanoparticles onto graphene nanosheets and showed obviously improved lithium storage performance (**Fig. 6a, b**).<sup>117</sup> The obtained composite exhibited a high specific capacity of 810 mAh g<sup>-1</sup> in the first cycle and 570 mAh g<sup>-1</sup> after 30 cycles, which was much better than the electrode with bare SnO<sub>2</sub>. In such a combination case, the pores formed between SnO<sub>2</sub> nanoparticles and graphene nanosheets can be used as the buffering space to accommodate the volume variation of SnO<sub>2</sub> nanoparticles during charge-discharge processes. In addition, the graphene nanosheets introduced can not only provide conductive channels for SnO<sub>2</sub> nanoparticles, but also synergistically contribute to the capacity. This pioneering research strongly suggests that the combination of 0D nanoparticles with 2D graphene is an efficient way to develop high-performance LIB anode materials. Specifically, this 2D/0D combination formula has recently induced the appearance of an amount of new composite electrode materials systems, such as anode materials involving SnO<sub>2</sub>,<sup>47, 68, 76, 104, 117-134</sup> Co<sub>3</sub>O<sub>4</sub>,<sup>84, 109, 135-140</sup> Fe<sub>3</sub>O<sub>4</sub>,<sup>69, 82, 141-147</sup> Fe<sub>2</sub>O<sub>3</sub>,<sup>80, 148-155</sup> Mn<sub>3</sub>O<sub>4</sub>,<sup>156-159</sup> MnO<sub>2</sub>,<sup>160, 161</sup> MoO<sub>3</sub>,<sup>162</sup> MoO<sub>2</sub>,<sup>163-165</sup> CuO,<sup>166</sup> NiO,<sup>167-169</sup> ZnO,<sup>170</sup> TiO<sub>2</sub>,<sup>171-174</sup> Sn,<sup>175-177</sup> Si,<sup>178-194</sup> Ge,<sup>195-198</sup> GeO<sub>x</sub>,<sup>199</sup> Li<sub>4</sub>Ti<sub>5</sub>O<sub>12</sub>,<sup>200</sup> CoFe<sub>2</sub>O<sub>4</sub><sup>201</sup> and CoSnO<sub>3</sub><sup>202</sup> as well as cathode materials involving sulfur,<sup>203-207</sup> LiFePO<sub>4</sub>,<sup>208-212</sup> FeF<sub>3</sub>,<sup>213</sup> and so on.

1D nanostructures are attractive candidates for LIB electrodes since they can be managed to provide efficient 1D pathway for fast electron transport, and facilitate strain relaxation at the same time. In spite of this, they still deliver the unsatisfactory electrochemical performances. Similar to the case of 0D nanoparticles, tremendous studies have been conducted with a focus on the structural engineering of such 1D/2D composites.<sup>38</sup> A variety of 1D nanostructures including nanowires (e.g. SnO<sub>2</sub>,<sup>214</sup> Si,<sup>55, 215-218</sup> Ge<sup>100</sup>, and TiO<sub>2</sub>,<sup>219</sup> V<sub>2</sub>O<sub>5</sub>,<sup>220-222</sup> AgVO<sub>3</sub>,<sup>223</sup>) nanorods (e.g. Sn,<sup>224</sup> SnO<sub>2</sub>,<sup>57, 225-227</sup> Fe<sub>3</sub>O<sub>4</sub>,<sup>228</sup> Co<sub>3</sub>O<sub>4</sub>,<sup>229</sup> MnO<sub>2</sub>,<sup>230-232</sup> Mn<sub>3</sub>O<sub>4</sub>,<sup>233</sup> MoO<sub>3</sub>,<sup>64</sup> ZnMn<sub>2</sub>O<sub>4</sub>,<sup>234</sup> LiMn<sub>1-x</sub>Fe<sub>x</sub>PO<sub>4</sub>,<sup>94</sup>) nanotubes (e.g. carbon,<sup>235</sup> TiO<sub>2</sub>,<sup>236</sup>) nanofibers (e.g. carbon,<sup>77</sup>) and core-shell nanocables (e.g. Sn@C,<sup>89</sup> Si@C,<sup>101</sup>, LiFePO<sub>4</sub>@C,<sup>237</sup>) have been developed and integrated with graphene sheets, forming 3D hybrid networks. For instance, recently, we developed a simple and efficient strategy to prepare Sn-core/carbon-sheath coaxial nanocables directly integrated onto the RGO surface by an RGO-mediated procedure (**Fig. 6c, d**).<sup>89</sup> The unique structure of such composites promises several advantageous features favourable for the anodes in LIBs. First, the carbon sheath of the nanocables acts as a physical barrier to protect the Sn core against

pulverization and simultaneously prevent the Sn cores of neighbouring nanocables from coalescing into bulk during charge-discharge processes. Second, the discrete nanocables with conductive carbon sheaths are interconnected through the underlying RGO matrix, thus facilitating fast electron transfer throughout the electrode. Third, the unique combination of 2D graphene and high-aspect-ratio 1D nanocables creates a large quantity of pores. This not only affords increased electrode-electrolyte contact area and facilitates fast transport of lithium ions, but also helps to accommodate the volume change of Sn during charge-discharge processes. As a result, a stable cycling of 50 cycles was observed and the specific capacity still remained at 630 mAh g<sup>-1</sup> based on the total mass of the composite, apparently superior to those of their counterparts without carbon sheaths and/or RGO supports.

Two-dimensional (2D) nanomaterials such as graphene and inorganic nanosheets/nanoplates have received much attention in recent years, because of their unusual properties associated with their ultrathin feature and 2D morphology.<sup>238-242</sup>

Accordingly, great efforts have been devoted to exploiting their potential applications in many fields including electronics, optoelectronics, energy storage devices, and so on.<sup>243-254</sup> By combining graphene and 2D electrochemically active inorganic substances, a series of various 2D/2D graphene based composite electrode materials have been developed for LIBs so far, either by *in situ* synthesis of 2D nanomaterials onto graphene nanosheets, or by self-assembly processes of as-synthesized 2D nanomaterials on graphene. According to their diverse components, the existing 2D nanomaterials composited with graphene can be classified into layered metal chalcogenides,<sup>58, 90, 255-266</sup> layered double hydroxides,<sup>267-270</sup> and non-layered metal,<sup>88</sup> metal oxide<sup>60, 95, 271-281</sup> or phosphate<sup>282</sup> nanosheets and/or nanoplates. Layered metal dichalcogenides, such as MoS<sub>2</sub>, SnS<sub>2</sub>, WS<sub>2</sub>, and TiS<sub>2</sub>, have been previously studied and employed in battery applications.<sup>283</sup> Recently, stacked MoS<sub>2</sub> nanosheets prepared from chemical lithiation and exfoliation have been emerging and attracting much attention.<sup>284</sup> Chang *et al.* synthesized graphene-layered MoS<sub>2</sub> nanocomposites (RGO-MoS<sub>2</sub>) by an L-cysteine-assisted hydrothermal process.<sup>255</sup> When used as LIB anode materials, the graphene-MoS<sub>2</sub> composite with a Mo: C molar ratio of 1: 2 exhibited the highest specific capacity of ~1100 mA h g<sup>-1</sup> at a current rate of 100 mA g<sup>-1</sup>, excellent cycling stability, and high rate capability (Fig. 6e, f). This is suggested to be attributed to a synergistic effect in the RGO-MoS<sub>2</sub> composites which enables the formation of short lithium ion diffusion channels, interconnected conductive network, and robust structural framework. Furthermore, other types of metal chalcogenides, including SnS<sub>2</sub>,<sup>59, 65, 261, 285-288</sup> In<sub>2</sub>S<sub>3</sub>,<sup>257, 289</sup> Sb<sub>2</sub>S<sub>3</sub>,<sup>256</sup> CoS,<sup>290</sup> Co<sub>3</sub>S<sub>4</sub>,<sup>291</sup> SnSe<sub>2</sub>,<sup>292</sup> have been studied as well and their composites with graphene consistently show obviously improved lithium storage performances including high specific capacity and good cycling stability.

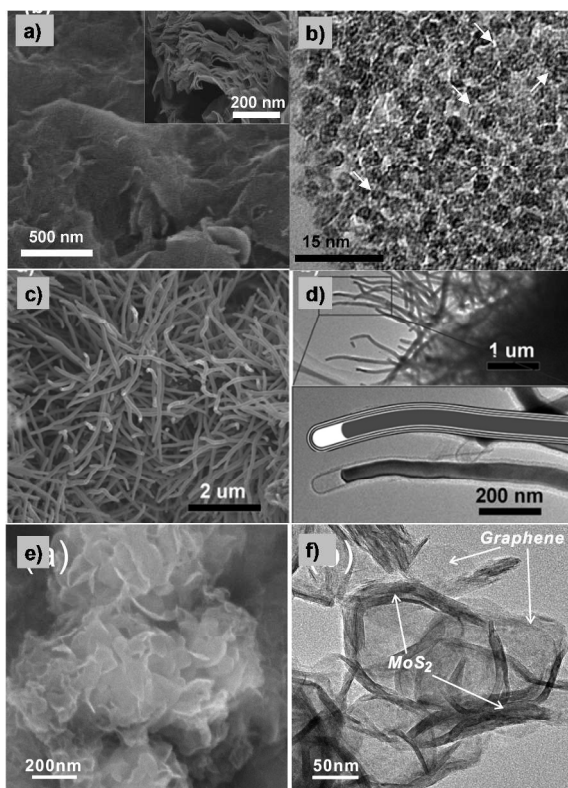


**Fig. 6** (a) Cross-sectional SEM and (b) TEM images for the graphene/SnO<sub>2</sub> nanoparticles composite. Reproduced with permission from ref.<sup>117</sup>. Copyright 2009, American Chemical Society. (c) SEM and (d) TEM images of the graphene supported 1D Sn-core/carbon-sheath coaxial nanocables composite. Reproduced with permission from ref.<sup>89</sup>. Copyright 2013, WILEY-VCH Verlag GmbH & Co. KGaA. (e) SEM and (f) TEM images of the graphene/MoS<sub>2</sub> composites. Reproduced with permission from ref.<sup>255</sup>. Copyright 2011, American Chemical Society.

### 3.2 Graphene Layer Orientation within the composite

It is well known that one of the major roles of graphene in a composite electrode material is to construct 3D conductive network, which effectively collect/transport charge carriers (e.g., electrons) from/to the active materials during the charge and discharge processes. Meanwhile, pore structures resulting from the interlinked graphene nanosheets have an important affect on the diffusion dynamics of lithium ion within the composite, which is one of the critical factors limiting the rate performance of the battery. Thus, a high quality 3D graphene network with reasonably arranged graphene layer is highly desirable to create good transport channels for both electrons and ions and thus lead to both high power and rate capabilities. According to the different direction to the surface of the electrode, the arrangement of graphene layer within the reported 3DGCs can be classified into three modes, including randomly oriented, parallelly aligned and vertically oriented graphene, as shown in Fig. 7a-c.

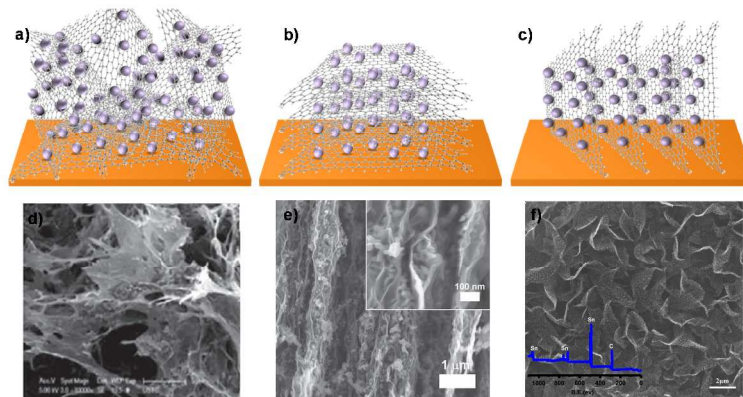


**Fig. 7** (a-c) Schematic illustration of three types of graphene arrangement modes in 3DGCs: a) randomly oriented graphene, b) parallelly aligned graphene and c) vertically oriented graphene. (d) SEM images of the cross-section of the as-prepared 3D graphene/Fe<sub>3</sub>O<sub>4</sub> aerogel (10000×). Reproduced with permission from ref. <sup>107</sup>. Copyright 2011, WILEY-VCH Verlag GmbH & Co. KGaA. (e) SEM image of the cross-section of a Si-graphene paper, the inset shows Si nanoparticles embedded between graphene sheets uniformly. Reproduced with permission from ref. <sup>181</sup>. Copyright 2011, WILEY-VCH Verlag GmbH & Co. KGaA. (f) SEM image of the Sn NPs@Graphene-vertically aligned graphene composites. The inset in (f) is the corresponding XPS spectrum. Reprinted with permission from ref. <sup>293</sup>. Copyright 2014, Elsevier.

### 3.2.1 Randomly oriented graphene

Many kinds of 3DGCs with randomly oriented graphene layer have been developed.<sup>37, 294</sup> One type of promising candidates to construct 3D graphene network is graphene derivatives such as GO and RGO due to their solution processibility and possibility for large scale production. Another benefit with RGO-based network should be the oxygen-containing functional groups, which can serve as appealing substrates for the binding of various organic or inorganic species, providing an opportunity for the construction of graphene-based porous composites with different complexity. Recently, various metal or metal oxide nanomaterials have been integrated onto 3D RGO-based network and employed as electrode for lithium ion storage.<sup>107, 136, 182, 295-297</sup> As demonstrated in one typical case, macroporous RGO aerogel loaded with Fe<sub>3</sub>O<sub>4</sub> particles (Fig. 7d) was prepared via an *in situ* self-assembly procedure and exhibited a high capacity of ~990 and ~730 mAh g<sup>-1</sup> even when the current density was 800 and 1600 mA g<sup>-1</sup>, respectively. The porous structure of the hybrids was considered to benefit the diffusion of electrolyte ions and to reduce the damage caused by the volume change of Fe<sub>3</sub>O<sub>4</sub> nanoparticles during charge-discharge cycles. Moreover, the robust 3D framework of graphene provided a highly conductive network with large surface area and short diffusion length for the transport of lithium ions.

Besides the RGO-based network derived from solution-based methods, 3D highly porous graphene networks also have been prepared through CVD techniques with porous metal substrates as templates<sup>298, 299</sup> and employed as substrate to deposit other nanomaterials.<sup>81, 300-302</sup> For example, Luo *et al.* reported a bottom-up strategy to graft bicontinuous mesoporous nanostructure Fe<sub>3</sub>O<sub>4</sub> onto 3D graphene foams

prepared by CVD method and directly use the composite as the lithium ion battery anode.<sup>300</sup> This electrode exhibits a high capacity of 785 mAh g<sup>-1</sup> at 1C rate without decay up to 500 cycles.

### 3.2.2 Parallelly aligned graphene

Due to its two dimensional nature, graphene materials are more likely to be assembled into layered structure, such as graphene film or paper, with parallelly aligned graphene nanosheets inside. Until now, great efforts have been devoted to prepare 3DGCs with parallelly aligned graphene, and some of them can be used as free-standing and binder-free electrodes. For instance, flexible graphene films were employed as current collectors, upon which active nanomaterials were attached by chemical deposition<sup>303</sup> or hydrothermal reaction.<sup>304</sup> Such approaches usually produce low loading and aggregation of active nanomaterials, resulting in quite limited property improvement as electrode. Another way is based on the vacuum filtration, by which various active materials (such as TiO<sub>2</sub>,<sup>305</sup> MnO<sub>2</sub>,<sup>306</sup> V<sub>2</sub>O<sub>5</sub>,<sup>221</sup> Co<sub>3</sub>O<sub>4</sub>,<sup>229, 307</sup> and silicon<sup>101, 215</sup>) were incorporated into graphenes. Specifically, both components were homogeneously mixed and filtered to produce paper-like electrodes. Within these structures, parallelly aligned graphene layers form a conductive network behaving as a mechanical support and an embedded-in current collector. However, rate performances of such paper-like composite electrodes are always limited due to the kinetic limitations of ion/electron transportation in the direction perpendicular to the paper surface. To address this issue, Zhao *et al.* introduced in-plane, nm-sized carbon vacancies into the aligned graphene sheets and sandwiched silicon nanoparticles between them (Fig. 7e).<sup>181</sup> Li ions in the resultant 3D composite network can diffuse easily across graphene sheets throughout the structure by passing through the in-plane vacancy defects. As a consequence, paper-like 3DGCs with a combination of power capability and storage capacity for battery electrode applications were obtained without sacrificing its mechanical properties.

### 3.2.3 Vertically oriented graphene

Another way to evade the ion/electron transfer kinetic limitation is to prepare GCs with vertically oriented graphene sheets, in which the ion transfer pathways can be shorted as illustrated in Fig. 7c. Very recently, vertically aligned graphene sheets on metal substrate have been developed via plasma enhanced chemical vapour deposition techniques,<sup>308-310</sup> and Li *et al.* anchored several kinds of active nanomaterials (e.g. Sn@graphene,<sup>293</sup> Si@graphene,<sup>311</sup> SnO<sub>2</sub> NPs,<sup>309</sup> and Sn@CNTs<sup>312</sup>) on the sides of graphene sheets. The vertically aligned graphene sheets sandwiched by the active nanomaterials can supply rapid transport pathways for both lithium ions and electrons and thus resulting in high rate performances. For instance, the *in situ* growth of Sn NPs@Graphene-vertically aligned graphene composites (Fig. 7f) exhibit a high capacity 1037 mAh g<sup>-1</sup> even after prolonged cycling, in addition to a coulombic efficiency in excess of 97 %, which reflects the ability of the Sn@graphene nanostructure to prevent the volume change and agglomeration of the Sn-NPs.<sup>293</sup> The cycling ability exceeds 5000 times in half-cells at a 6C rate while retaining 400 mAh g<sup>-1</sup> reversible capacities. The excellent electrochemical performance observed is mainly attributed to the confined volume change of the Sn within the graphene, ensuring the permanent electrical connectivity of the immobilized Sn@graphene anodes.

### 3.3 Interfacial contact between graphene and active nanomaterials

As mentioned above, graphenes within 3DGCs play an important role in collecting electrons from the active nanomaterials during charge-discharge process. Therefore, a high-quality interfacial contact between graphene and the active materials is also highly desirable to reduce the contact resistance between them.

Taking into account the size of the active nanomaterials relative to the lateral size and the flexible nature of graphene, the combination strategy can usually result in two types of graphene-based composite electrode materials: graphene-supported composite and graphene-encapsulated composites. Theoretically, the contact surface between graphene and the second components of the later structure should be larger than the former type, and thus the graphene-encapsulated composite structure could be more stable to avoid the exfoliation of the second components from the graphene sheets. In this structure, graphene functioned as protection layer, which could more effectively prevent the aggregation of the second components in comparison with the graphene-supported nanocomposites. A variety of graphene-encapsulated nanocomposites, including graphene wrapped nanoparticles<sup>109, 180, 208, 313, 314</sup>, hollow particles<sup>315</sup> and nanowires<sup>100, 214, 216, 217</sup>, have been fabricated for high-performance lithium storage electrode materials. For example, graphene-encapsulated Co<sub>3</sub>O<sub>4</sub> nanoparticles hybrid architecture can not only suppress the aggregation of oxide nanoparticles, but accommodate the volume change during the cycle processes, and thus exhibits a very high reversible capacity of over 1000 mAh g<sup>-1</sup> after 130 cycles.<sup>109</sup> Luo *et al.* developed crumpled graphene-encapsulated Si nanoparticles via a one-step capillary-driven assembly route (**Fig. 8a**).<sup>180</sup> The folds and wrinkles in the crumpled graphene coating can accommodate the volume expansion of Si upon lithiation without fracture, and thus help to protect Si nanoparticles from excessive deposition of the insulating solid electrolyte interphase. Compared to the native Si particles, the composite capsules have greatly improved performance as Li ion battery anodes in terms of capacity, cycling stability, and Coulombic efficiency. From the dimensional point of view, it is worth mentioning that the 1D nanomaterials<sup>38</sup> (e.g. nanotubes, nanorods, nanowires) and 2D nanomaterials<sup>316</sup> (e.g. nanosheets, nanoplates, nanofilm) could be either grown vertically on graphene nanosheets<sup>55</sup>, or parallelly deposited on them.<sup>307, 317-319</sup> One of the most exciting cases is the surface-to-surface combination between graphene nanosheets and the both sides of a 2D component. This 2D/2D combination formula enables the exertion of the respective functions of both components, representing a smart prototype of new electrode material architectures. For that the sandwiched 2D component is elaborately endowed with dual efficient channels for fast transport of both electrons and lithium ions, which is highly desirable for the development of high-performance lithium-ion batteries. Recently, we demonstrated an elegant strategy to synthesize graphene-2D Sn nanocomposites (**Fig. 8a, b**), in which Sn nanosheets were sandwiched between graphene nanosheets. The thus-constructed 2D/2D composite material exhibited high reversible capacity as well as excellent cycling performance (>590 mA h g<sup>-1</sup> after 60 cycles), demonstrating great potential as anode materials in LIBs (**Fig. 8c**). The significantly improved lithium storage performances achieved are believed to be mainly originated from the 2D/2D sandwich structure of graphene and tin nanosheets. The graphene layer on both sides of Sn nanosheets not only avert the adjacent Sn nanosheets from coalescing together, but also afford channels for fast electron transport in view of their surface-to-surface

contacts.

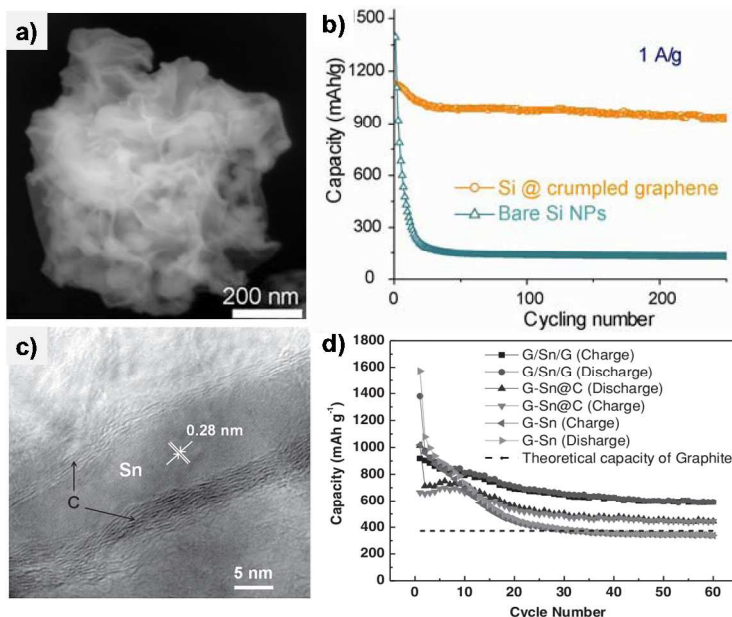


**Fig. 8** (a) SEM image of a single capsule of graphene-wrapped Si. (b) charge/discharge cycling test of the composite capsules in comparison to the unwrapped Si nanoparticles at a constant current density of 1 A/g. Reproduced with permission from ref.<sup>180</sup>. Copyright 2012, American Chemical Society. (c) TEM image and (d) electrochemical performance of the graphene-confined tin nanosheets. Reproduced with permission from ref.<sup>36</sup>. Copyright 2012, WILEY-VCH Verlag GmbH & Co. KGaA.

#### 10 3.4 Interfacial contact with the electrolyte

Compared to other carbonaceous substrates such as graphite, carbon black, and carbon nanotubes, graphene nanosheets can more effectively buffer the strain from the volume change of active materials during the charging-discharging processes and preserve the high electrical conductivity of the overall electrode. Nevertheless, the exposed active nanomaterials on the graphene surface are still prone to disintegrate or break down and, meanwhile, the volume expansion and aggregation of these active materials are difficult to be avoided.<sup>76</sup> For example, recently, a self-supported anode material consisting of silicon nanowires (SiNWs) sandwiched in between RGO nanosheets was prepared by vacuum filtration of an aqueous dispersion of GO with SiNWs followed by thermal annealing.<sup>215</sup> Within the 2D/1D composite anode architecture (namely, SiNW@RGO), SiNWs are packed by mechanically robust and flexible RGO nanosheets capable of accommodating the large volume expansion of embedded Si, thus allowing the direct use of the as-prepared SiNW@RGO composite material as a self-supported electrode without addition of any additives. As a consequence, the SiNW@RGO composite exhibited high reversible capacity of ca. 3350 mA h g<sup>-1</sup>, on the basis of the silicon mass. However, it was found that this high capacity could only stay for 25 cycles. Further characterization of the cycled composite materials showed that the graphene-packed

SiNWs bore a porous morphology with a sponge-like structure, which was assumed to mainly originate from the direct contact of Si with the electrolyte and the repeated formation of SEI layers. These negative factors can lead to a decreased electrochemical performance of graphene based composites.

Therefore, it is highly desirable to develop 3DGCs with unique structures that can tackle the aggregation of active nanomaterials while keeping the overall electrode highly conductive and active in lithium storage. Recently, many efforts have been devoted to this issue and several strategies, such as surface modification<sup>78, 122, 124, 320-323</sup>, pre-encapsulation<sup>101, 295</sup>, have been developed to meliorate the interfacial contact between the composite and electrolyte. For instance, very recently, a hierarchical 2D/1D architecture of RGO-sandwiched Si@C nanocables (**Fig. 9a**) was designed to address the interfacial stability issue of Si nanowires.<sup>101</sup> The pre-loaded carbon shell, together with the flexible and conductive RGO overcoats, synergistically accommodate the volume change of embedded SiNW@G nanocables and thus maintain the structural and electrical integrity of the composite. The adaptable nature of this composite completely prohibits the fuse and aggregation of the neighboring SiNWs upon cycling, effectively prevents the direct contact of silicon with the electrolyte, efficiently averts the pore formation in silicon, and thus secures the integrity of SiNWs during repeated cycling. Such a structural and interfacial engineering formula of Si endowed the electrodes with significantly improved lithium storage performances (Fig. 9c) when compared to their counterparts; specifically, such composites possess high reversible specific capacity of 1600 mA h g<sup>-1</sup> at 2.1 A g<sup>-1</sup>, 80% capacity retention after 100 cycles, and superior rate capability (500 mA h g<sup>-1</sup> at 8400 A g<sup>-1</sup>). The strategy demonstrated for the protection of Si with dual adaptable substances opens a new door for developing Si-based anodes for advanced LIBs from a view point of materials system engineering. In another case, Wei *et al.* fabricated 3D graphene foams cross-linked with Fe<sub>3</sub>O<sub>4</sub> nanospheres (NSs) encapsulated with graphene. Such hierarchical Fe<sub>3</sub>O<sub>4</sub>/graphene hybrids provide double protection against the volume changes of Fe<sub>3</sub>O<sub>4</sub> NSs during electrochemical processes.<sup>295</sup> The graphene shells suppress the aggregation of Fe<sub>3</sub>O<sub>4</sub> NSs and buffer the volume expansion of 3D graphene foams cross-linked with pre-encapsulated Fe<sub>3</sub>O<sub>4</sub> nanospheres, while the interconnected 3D graphene networks act to reinforce the core-shell structure of Fe<sub>3</sub>O<sub>4</sub>@GS and thus enhance the electrical conductivity of the overall electrode. As a result, Fe<sub>3</sub>O<sub>4</sub>@GS/graphene delivers a high reversible capacity of 1059 mAh g<sup>-1</sup> over 150 cycles, and excellent rate capability, thus exhibiting great potential as an anode material for lithium storage.

Graphene wrapping layer has been demonstrated to efficiently buffer the strain from the volume change of active materials and preserve high electrical conductivity. However, when considering the ion diffusion efficiency within 3DGCs, graphene layer might play a negative role as the Li<sup>+</sup> diffusion through a defect-free graphitic plane is limited.<sup>324, 325</sup> For instance, Wei *et al.* reported that a partial graphene wrapping provides a balance between increased electron transport and fast ion diffusion while full graphene wrapping isolates LiFePO<sub>4</sub> from the electrolyte and retards ion diffusion.<sup>326</sup> Therefore, a good steric hindrance for ion diffusion should also be considered together with electron transport in constructing 3DGCs for high power LIBs.

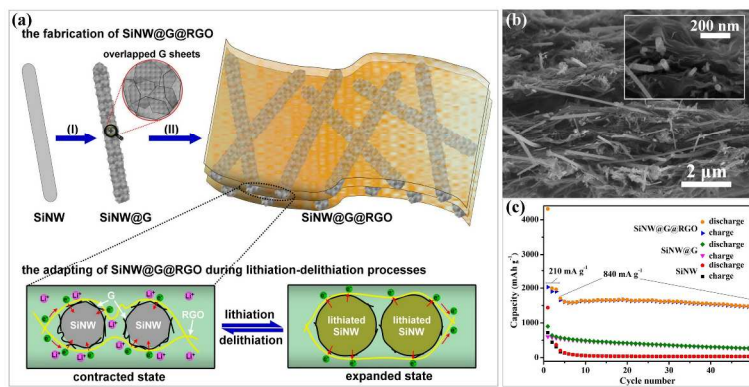


**Fig. 9** (a) Schematic illustration of the fabrication (upper panel) and adapting (lower panel) of SiNW@G@RGO. (b) cross-section SEM image of SiNW@G@RGO with an enlarged view in the inset. (c) Comparison of capacity retention of different electrodes. Reproduced with permission from ref.<sup>101</sup>. Copyright 2013, American Chemical Society.

#### 4 Summary and Outlook

In this review, we have summarized the recent progress in 3D graphene-based composites, with a focus on the rational structural and interface design of 3DGCs <sup>10</sup> electrode materials for lithium ion batteries. By exemplifying the combination of graphene with other active nanomaterials, we highlight the importance of the dimensional matching and interfacial engineering in the design and construction of graphene-involved composites for LIB applications, providing more scientific insights into the smart knitting of electrochemically active LIB electrode materials <sup>15</sup> with graphene for the development of high performance LIBs. The electrochemical performance of different kinds of graphene-based composite electrode materials are summarized and compared in **Table 1**. Different electrode materials have their own advantages and shortcomings. In terms of the practical application in LIBs, although enhanced cycling performance and/or improved specific capacity of 3DGCs have <sup>20</sup> been reported in most cases, more attention should be paid on some other crucial performances of an electrode material, e.g., initial efficiency, volumic energy density and power density. For example, high porosity of 3DGCs might be beneficial to relieve the volume effect and accelerate ion diffusion, while also lead to low initial efficiency and poor compact density and thus low volumic energy <sup>25</sup> density. Moreover, in most cases graphene wrapping or encapsulating can strengthen the electronic conductivity and the mechanical stability of the electrode, whereas its limitation to ion diffusion should not be ignored when designing 3DGCs for LIBs. Therefore, rational design on the pore structure and Interfacial contact within the <sup>30</sup> 3DGCs are crucial to find a balance between the electrochemical performances according to the different practical requirements.

Although lots of strategies on the construction of 3DGCs with specific morphologies have been demonstrated, there is still a long way to go. Experimental results achieved so far on the dimensional-fitting combination and effective interfacial engineering of graphene and electrochemically active nanomaterials have <sup>35</sup> just opened up a new avenue for the development of high performance electrode

materials. Scientific details, particularly the dimensional-fitting effects, the interface-property relationship, the ion/electron transport mechanism, and so on, are still waiting for systematic and deeper exploration. In addition, feasible strategies towards well-defined structural and interfacial engineering, economic and scalable production, and green and convenient integration of these 3DGCs have to be carefully addressed as well before being implemented as competitive commercial building blocks in practical energy storage applications.

CREATED USING THE RSC REPORT TEMPLATE (VER. 3.1) - SEE WWW.RSC.ORG/ELECTRONICFILES FOR DETAILS

REVIEW

www.rsc.org/xxxxxx | XXXXXXXX

**Table 1.** Electrochemical performance comparison of some representative 3DGCs for lithium ion batteries.

Active component	3D Graphene based Composites	Capacity (mAh g <sup>-1</sup> )	Cycles	Current density (mA g <sup>-1</sup> )	Voltage window (V)	Year	Ref.
Tin	Sn/graphene nanocomposite	508	100	55	0.01-3.0	2009	175
	Graphene supported Sn-Sb@C core-shell particles	978	30	0.1C	0.005-3.0	2010	176
		668		2C			
	Sn-graphene	794	400	C/3	0.01-3.0	2011	297
	Multilayered graphene/Sn-nanopillar nanostructure	679	30	50	0.002-3.0	2011	224
		408		5000			
	Tin-graphene nanocomposites	542	30	1600	0.005-3.0	2012	327
	Graphene-confined Sn nanosheets	590	60	50	0.005-2.0	2012	328
	RGO-Sn@C nanocables	630	50	100	0.005-2.5	2012	89
	N-doped graphene encapsulated Sn NPs	481	100	100	0.005-2.0	2013	329
		307		2000			
	Sn@C embedded graphene nanosheet composites	566	100	75	0.01-3.0	2013	328
	Sn/Graphene Composite	600	20	100	0.02-1.2	2014	330
Tin oxide	Sn@CNTs on vertically aligned graphene	1013	200	0.25C	0.001-3.0	2014	311
		164		300C			
	Sn@graphene on vertically aligned graphene	1005	120	150	0.001-3.0	2014	293
		400	5000	400			
	Graphene networks anchored with Sn@Graphene	1022	100	0.2C	0.005-3.0	2014	177
		682	1000	2000			
	SnO <sub>2</sub> /Graphene nanoporous composites	570	30	50	0.05-2.0	2009	117
	SnO <sub>2</sub> -G composite	558	60	264	0.01-3.0	2010	126
	Ordered metal oxide/graphene nanocomposites	760	100	8	0.02-1.5	2011	120

[journal], [year], [vol], 00–00 | 18

This journal is © The Royal Society of Chemistry [year]

CREATED USING THE RSC REPORT TEMPLATE (VER. 3.1) - SEE WWW.RSC.ORG/ELECTRONICFILES FOR DETAILS

Active component	3D Graphene based Composites	Capacity (mAh g <sup>-1</sup> )	Cycles	Current density (mA g <sup>-1</sup> )	Voltage window (V)	Year	Ref.
	SnO <sub>2</sub> /graphene composites	550 460	100	0.2C 5C	0.005-2.0	2011	331
	SnO <sub>2</sub> /graphene nanocomposite	1304	150	100	0.01-3.0	2011	332
	SnO <sub>2</sub> /graphene composite	840 590	30 50	67 400	0.01-2.0	2011	333
	Graphene enwrapped SnO <sub>2</sub> hollow nanospheres	696 307	300	500 5000	0.005-3.0	2012	121
	SnO <sub>x</sub> -carbon-graphene nanocomposites	565	50	200	0.01-2.0	2012	334
	Monodisperse SnO <sub>2</sub> nanorods on graphene	710	50	100	0.005-3.0	2012	57
	SnO <sub>2</sub> Nanocrystals in Nitrogen-Doped Graphene Sheets	1021	500	500	0.005-3.0	2013	335
	RGO/SnO <sub>2</sub> composite	717 512	200	100 1000	0.01-2.0	2013	336
	SnO <sub>2</sub> nanoparticles entrapped in a graphene framework	500	50	100	0.01-3.0	2013	296
	SnO <sub>2</sub> /graphene composites	872	200	100	0.01-2.5	2013	337
	Graphene nanoribbon / SnO <sub>2</sub> NPs composite	825	50	100	0.01-2.5	2013	128
	SnO <sub>2</sub> nanoparticles anchored on vertically aligned graphene	996 210	100 5000	80 9000	0.001-3.0	2014	309
	SnO <sub>2</sub> /graphene composites	1024 550	50	100 10000	0.02-3.0	2014	338
Transition metal oxide	Graphene-Wrapped Fe <sub>3</sub> O <sub>4</sub>	1026 580	30 100	35 700	0.001-3	2010	82
	Fe <sub>3</sub> O <sub>4</sub> -graphene nanocomposite	1048	90	100	0.01-3.0	2010	339
	Graphene-Encapsulated Hollow Fe <sub>3</sub> O <sub>4</sub> Nanoparticle	832	90	100	0-3.0	2011	143

[journal], [year], [vol], 00–00 | 19

This journal is © The Royal Society of Chemistry [year]

CREATED USING THE RSC REPORT TEMPLATE (VER. 3.1) - SEE WWW.RSC.ORG/ELECTRONICFILES FOR DETAILS

Active component	3D Graphene based Composites	Capacity (mAh g <sup>-1</sup> )	Cycles	Current density (mA g <sup>-1</sup> )	Voltage window (V)	Year	Ref.
Metal chalcogenide	Fe <sub>3</sub> O <sub>4</sub> -Carbon-RGO three dimensional composite	842	100	200		2011	144
	Graphene-Encapsulated Fe <sub>3</sub> O <sub>4</sub> Nanoparticles	650	100	100	0-3.0	2011	141
	Fe <sub>3</sub> O <sub>4</sub> -graphene nanocomposites	1280	100	0.1C		2011	340
		860		4C			
	Hollow porous Fe <sub>3</sub> O <sub>4</sub> beads-RGO composites	1039	170	100	0.005-3.0	2012	69
	3D Graphene Foam Supported Fe <sub>3</sub> O <sub>4</sub>	785	500	1C	0.01-3.0	2013	300
	3D Graphene Foams Cross-linked with Pre-encapsulated Fe <sub>3</sub> O <sub>4</sub> Nanospheres	1059	150	93	0.01-3.0	2013	295
		363		4800			
	Fe <sub>3</sub> O <sub>4</sub> nanorod graphene composites	867	100	1C	0.01-3.0	2013	228
		569		5C			
	Fe <sub>3</sub> O <sub>4</sub> -Coated Three-Dimensional Graphene	864	50	200	0.01-3.0	2014	81
	Graphene@ $\alpha$ -Fe <sub>2</sub> O <sub>3</sub> core-shell NPs	781	100	200	0.01-3.0	2011	214
	Graphene sandwiched $\alpha$ -Fe <sub>2</sub> O <sub>3</sub> hexagonal nanoplatelets	1100	50	0.2C	0.005-3.0	2013	341
		887		1C			
	Fe <sub>3</sub> O <sub>4</sub> -SnO <sub>2</sub> -graphene ternary nanocomposite	1198	115	100	0.01-3.0	2011	342
Metal chalcogenide	Graphene-encapsulated Co <sub>3</sub> O <sub>4</sub> nanoparticles	1000	130	74	0.01-3.0	2010	109
	Co <sub>3</sub> O <sub>4</sub> /graphene hybrid	800	40	200	0.01-3.0	2011	
		550		1000			
	Graphene encapsulated mesoporous Co <sub>3</sub> O <sub>4</sub> composite	820	35	100	0.01-3.0	2012	138
	Two dimensional graphene-SnS <sub>2</sub> hybrids	650	30	50	0.01-1.3	2012	268
Metal chalcogenide		230		6400			
	Few-layer SnS <sub>2</sub> /graphene hybrid	920	40	100	0.01-1.5	2012	287
		600		1000			

Active component	3D Graphene based Composites	Capacity (mAh g <sup>-1</sup> )	Cycles	Current density (mA g <sup>-1</sup> )	Voltage window (V)	Year	Ref.
Silicon	SnS <sub>2</sub> @graphene nanocomposites	504	200	0.5C	0.05-1.0	2012	59
	SnS <sub>x</sub> -graphene nanocomposites	860	150	0.2C	0.02-2.5	2012	343
	SnS <sub>2</sub> @reduced graphene oxide nanocomposites	564	60	120	0.01-3.0	2012	261
	RGO-supported SnS <sub>2</sub> nanosheets	896	40	0.1C	0.01-3.0	2013	344
	Ultrathin SnS <sub>2</sub> Nanoplates on Graphene	704	100	0.6C	0.01-3.0	2013	285
	MoS <sub>2</sub> /graphene nanosheet composites	1290	50	100	0.1-3.0	2011	58
	Single-layer MoS <sub>2</sub> /graphene @ amorphous carbon	1116	250	100	0.01-3.0	2011	258
		850		1000			
	MoS <sub>2</sub> -coated three-dimensional graphene network	877	50	100	0.01-3.0	2013	345
		665	50	500			
	Graphene-like MoS <sub>2</sub> /graphene composites	940-1020	100	100	0.005-3.0	2013	66
	SnSe <sub>2</sub> nanoplate-graphene composite	640	30	40	0.01-3.0	2011	292
	Nanosize silicon/graphene composite	1168	30	100	0.01-1.2	2010	346
	Graphene-silicon composite film	708	100	50	0.02-1.2	2010	179
	Silicon nanoparticles-graphene paper composites	1500	200	100	0.02-1.5	2010	183
	Si-Graphene Composite	2600	150	1000	0.02-1.5	2011	181
		540	150	8000			
	Nanosilicon-coated graphene granules	~1060	150	1400	0.01-1.0	2011	78
	Si-Ph-G nanocomposite	828	50	200	0.01-3.0	2012	178
	Si nanowires in graphene papers	1400	30	420	0.005-1.5	2012	55
	Si/graphene nanocomposite	1000	30	100	0.01-2.0	2012	182
	Graphene/Si multilayer structure	1320	30	50	0.002-2.8	2012	347
	Crumpled graphene-encapsulated Si NPs	940	250	1000	0.02-2.0	2012	180

CREATED USING THE RSC REPORT TEMPLATE (VER. 3.1) - SEE WWW.RSC.ORG/ELECTRONICFILES FOR DETAILS

Active component	3D Graphene based Composites	Capacity (mAh g <sup>-1</sup> )	Cycles	Current density (mA g <sup>-1</sup> )	Voltage window (V)	Year	Ref.
Si/graphene composite	3D Graphene based Composites	1200		200			
	Si/graphene composite	1374	120	100	0.01-3.0	2013	348
	RGO-sandwiched SiNWs	3350	20	0.2C	0.002-2.0	2013	215
		1200		2C			
	RGO sandwiched Silicon-Carbon Nanocables	1280	100	2100	0.002-2.0	2013	101
		500		8400			
	3D graphene scaffold supported Si electrode	1310	50	797	0.01-1.5	2013	317
		1083	1200	2930			
	Si@C/graphene nanocomposite	1410	100	500	0.01-2.0	2014	349
	3D SiOx/C@RGO nanocomposite	1284	100	100	0.01-1.5	2014	350
Other anodes	Silicon/graphene based nanocomposite	866	200	0.4 mA cm <sup>-2</sup>	0.02-2.0	2014	351
	Graphene encapsulated silicon nanoparticles/vertically aligned graphene	1021	150	150	0.001-1.0	2014	312
		412		8000			
	Sandwich-structured C/Ge/graphene nanocomposite	993	160	0.4C	0.01-1.5	2013	352
	Graphene-encapsulated Ge nanowires	1400	50	1600	0.01-1.2	2013	100
	Co(OH) <sub>2</sub> graphene nanosheets composite	910	30	200	0.005-3.0	2010	269
	Hollow Structured Li <sub>3</sub> VO <sub>4</sub> wrapped with graphene nanosheets	345	50	20	0.2-3.0	2013	315
		223		8000			
	Nano-structured LiFePO <sub>4</sub> /graphene composites	160	80	0.2C	2.4-4.2	2010	353
		110		10C			
Lithium iron phosphate	LiMn <sub>1-x</sub> Fe <sub>x</sub> PO <sub>4</sub> nanorods grown on graphene sheets	155	100	0.2C		2011	94
		132		20C			
		107		50C			

Active component	3D Graphene based Composites	Capacity (mAh g <sup>-1</sup> )	Cycles	Current density (mA g <sup>-1</sup> )	Voltage window (V)	Year	Ref.
Sulfur (S weight percent)	Graphene modified LiFePO <sub>4</sub>	148 70		0.1C 60C	2.0-4.2	2011	354
	3D porous LiFePO <sub>4</sub> /graphene hybrid cathodes	146	100	17	2.5-4.2	2012	355
	Graphene wrapped LiFePO <sub>4</sub> /C composites	165	60	0.1C	2.0-4.2	2012	210
		88		10C			
	LiFePO <sub>4</sub> -graphene	160	100	17	2.5-4.2	2013	209
	Nano LiFePO <sub>4</sub> in RGO framework	152	50	0.2C	2.5-4.5	2014	356
	LiFePO <sub>4</sub> NPs encapsulated in graphene nanoshells	122	1000	170	2.0-4.3	2014	208
		84		1700			
	Graphene-wrapped Sulfur particles (70 %)	600	100	0.2C	1.6-2.5	2011	207
	Sulfur/Graphene nanocomposite (44.5 %)	819	100	0.05C	1.0-3.0	2012	357
		662	100	1C			
	Graphene-enveloped sulfur (87 %)	~500	50	0.2C	1.5-3.0	2012	358
	Carbon-sulfur nanocomposite coated with RGO (63 %)	928	100	200	1.0-3.0	2012	359
	Sulfur/hierarchical porous graphene (66 %)	1068	80	0.5C	1.5-3.0	2013	360
		543		10C			
	Porous activated graphene nanosheets/sulfur (67 %)	1379 685	60 100	0.2C 1C	1.0-3.0	2013	361
	Graphene-sulfur composites (73 %)	615	100	1C	1.5-3.0	2013	204
		570		2C			
	Polydopamine coated RGO/S composite (82 %)	728 530	500 800	500 1000	1.5-2.8	2013	362
	Fibrous hybrid of graphene and sulfur (63 %)	541	100	750	1.5-2.8	2013	203
	Amylopectin wrapped GO-S composite	441	175	5C/16	1.6-2.8	2013	363

CREATED USING THE RSC REPORT TEMPLATE (VER. 3.1) - SEE WWW.RSC.ORG/ELECTRONICFILES FOR DETAILS

Active component	3D Graphene based Composites	Capacity (mAh g <sup>-1</sup> )	Cycles	Current density (mA g <sup>-1</sup> )	Voltage window (V)	Year	Ref.
	Graphene sandwiched MWCNT@sulfur (70 %)	844	100	0.2C	1.0-3.0	2013	364
	Sulfur-infiltrated graphene-based porous carbon (68 %)	619	100	0.5C	1.7-2.6	2014	365
		583		5C			
	Graphene- Sulfur sandwich structure	950	100	750	1.5-2.8	2014	366
		680	300	1500			
Other cathodes	Li <sub>3</sub> V <sub>2</sub> (PO <sub>4</sub> ) <sub>3</sub> /graphene nanocomposites	128	50	0.1C	3.0-4.3	2011	367
		109	100	20C			
	LiNi <sub>1/3</sub> Co <sub>1/3</sub> Mn <sub>1/3</sub> O <sub>2</sub> graphene composite	185	25	0.05C	2.5-4.4	2011	368
		153		5C			
	LiMn <sub>2</sub> O <sub>4</sub> -graphene composite	123	80	0.2C	3.3-4.4	2011	157
	Rutile TiO <sub>2</sub> -Graphene Hybrid	170	100	1C	1.0-3.0	2009	174
	Anatase TiO <sub>2</sub> -Graphene Hybrid	160	100	1C			
	Graphene-based titania nanosheets	162		1C	1.0-3.0	2011	318
		123		10C			
	TiO <sub>2</sub> -reduced graphene oxide composite	152	100	5C	0.001-3.0	2012	171
	TiO <sub>2</sub> nanocrystals/RGO sheets	189	100	100	1.0-3.0	2013	79
		94		10000			
	Mesoporous TiO <sub>2</sub> nanocrystals@graphene aerogels	202	60	100		2014	52
		99		5000			
	Graphene-supported Li <sub>4</sub> Ti <sub>5</sub> O <sub>12</sub> nanosheets	201	100	1C	1.0-2.5	2012	95
		141		20C			
	V <sub>2</sub> O <sub>5</sub> nanowire/graphene composite	190	50	400	1.5-4.0	2011	220
	Ultra-thin V <sub>2</sub> O <sub>5</sub> nanowire-graphene composite	230	200	100	1.7-3.8	2012	221

CREATED USING THE RSC REPORT TEMPLATE (VER. 3.1) - SEE WWW.RSC.ORG/ELECTRONICFILES FOR DETAILS

Active component	3D Graphene based Composites	Capacity (mAh g <sup>-1</sup> )	Cycles	Current density (mA g <sup>-1</sup> )	Voltage window (V)	Year	Ref.
	VO <sub>2</sub> /graphene ribbons	415	210	1C	1.5-3.5	2013	70
		204	1000	190C			

[journal], [year], [vol], 00–00 | 25

This journal is © The Royal Society of Chemistry [year]

## Acknowledgements

The authors acknowledge the support from the Ministry of Science and Technology of China (No.2012CB933403), the National Natural Science Foundation of China (Grant No. 21173057, 21273054), the Beijing Municipal Science and Technology Commission (Z121100006812003), and the Chinese Academy of Sciences.

## References

- <sup>10</sup> <sup>a</sup> National Center for Nanoscience and Technology, Zhongguancun, Beiyitiao No.11, 100190, Beijing, P.R. China. Fax: +86 10 82545578; Tel: +86 10 82545578; E-mail: zhlf@nanoctr.cn
- 1 A. K. Geim and K. S. Novoselov, *Nat. Mater.*, 2007, **6**, 183-191.
  - 2 A. K. Geim, *Science*, 2009, **324**, 1530-1534.
  - 3 K. S. Kim, Y. Zhao, H. Jang, S. Y. Lee, J. M. Kim, K. S. Kim, J.-H. Ahn, P. Kim, J.-Y. Choi and B. H. Hong, *Nature (London)*, 2009, **457**, 706-710.
  - 4 V. C. Tung, M. J. Allen, Y. Yang and R. B. Kaner, *Nat. Nanotechnol.*, 2009, **4**, 25-29.
  - 5 X. L. Li, X. R. Wang, L. Zhang, S. W. Lee and H. J. Dai, *Science*, 2008, **319**, 1229-1232.
  - 6 D. C. Elias, R. R. Nair, T. M. G. Mohiuddin, S. V. Morozov, P. Blake, M. P. Halsall, A. C. Ferrari, D. W. Boukhvalov, M. I. Katsnelson, A. K. Geim and K. S. Novoselov, *Science*, 2009, **323**, 610-613.
  - 7 R. F. Service, *Science*, 2009, **324**, 875-877.
  - 8 S. Stankovich, D. A. Dikin, G. H. B. Domke, K. M. Kohlhaas, E. J. Zimney, E. A. Stach, R. D. Pineri, S. T. Nguyen and R. S. Ruoff, *Nature*, 2006, **442**, 282-286.
  - 9 R. R. Nair, P. Blake, A. N. Grigorenko, K. S. Novoselov, T. J. Booth, T. Stauber, N. M. R. Peres and A. K. Geim, *Science*, 2008, **320**, 1308-1308.
  - 10 V. Singh, D. Joung, L. Zhai, S. Das, S. I. Khondaker and S. Seal, *Prog. Mater. Sci.*, 2011, **56**, 1178-1271.
  - 11 X. Cao, Z. Yin and H. Zhang, *Energy Environ. Sci.*, 2014, **7**, 1850-1865.
  - 12 L. L. Jiang and Z. J. Fan, *Nanoscale*, 2014, **6**, 1922-1945.
  - 13 I. V. Lightcap and P. V. Kamat, *Accounts Chem. Res.*, 2013, **46**, 2235-2243.
  - 14 T. Qiu, B. Luo, M. Liang, J. Ning, B. Wang, X. Li and L. Zhi, *Carbon*, DOI: 10.1016/j.carbon.2014.09.054.
  - 15 X. Huang, X. Qi, F. Boey and H. Zhang, *Chem. Soc. Rev.*, 2012, **41**, 666-686.
  - 16 C. Xu, B. Xu, Y. Gu, Z. Xiong, J. Sun and X. S. Zhao, *Energy Environ. Sci.*, 2013, 1388-1414.
  - 17 B. Luo, S. Liu and L. Zhi, *Small*, 2012, **8**, 630-646.
  - 18 S. Bai and X. Shen, *Rsc Adv.*, 2012, **2**, 64-98.
  - 19 D. Wei and J. Kivioja, *Nanoscale*, 2013, **5**, 10108-10126.
  - 20 D. Chen, L. H. Tang and J. H. Li, *Chem. Soc. Rev.*, 2010, **39**, 3157-3180.
  - 21 M. Pumera, *Energy Environ. Sci.*, 2011, **4**, 668-674.
  - 22 Y. Sun, Q. Wu and G. Shi, *Energy Environ. Sci.*, 2011, **4**, 1113-1132.
  - 23 J. M. Tarascon and M. Armand, *Nature*, 2001, **414**, 359-367.
  - 24 C. Liu, F. Li, L. P. Ma and H. M. Cheng, *Adv. Mater.*, 2010, **22**, E28-E62.
  - 25 H. Li, Z. X. Wang, L. Q. Chen and X. J. Huang, *Adv. Mater.*, 2009, **21**, 4593-4607.
  - 26 M. G. Kim and J. Cho, *Adv. Funct. Mater.*, 2009, **19**, 1497-1514.
  - 27 K. T. Lee and J. Cho, *Nano Today*, 2011, **6**, 28-41.
  - 28 J. Zhu, D. Yang, Z. Yin, Q. Yan and H. Zhang, *Small*, 2014, 3480-3498.
  - 29 M. M. Atabaki and R. Kovacevic, *Electron. Mater. Lett.*, 2013, **9**, 133-153.
  - 30 M. H. Liang, B. Luo and L. J. Zhi, *Int. J. Energ. Res.*, 2009, **33**, 1161-1170.
  - 31 G. Kucinskis, G. Bajars and J. Kleperis, *J. Power Sources*, 2013, **240**, 66-79.
  - 32 M. H. Liang and L. J. Zhi, *J. Mater. Chem.*, 2009, **19**, 5871-5878.
  - 33 S. Xin, Y. G. Guo and L. J. Wan, *Accounts Chem. Res.*, 2012, **45**, 1759-1769.
  - 34 J. Liu, Y. Xue, M. Zhang and L. Dai, *Mrs. Bull.*, 2012, **37**, 1265-1272.
  - 35 X. Huang, Z. Yin, S. Wu, X. Qi, Q. He, Q. Zhang, Q. Yan, F. Boey and H. Zhang, *Small*, 2011, **7**, 1876-1902.
  - 36 N. Li, M. H. Cao and C. W. Hu, *Nanoscale*, 2012, **4**, 6205-6218.
  - 37 H. X. Chang and H. K. Wu, *Energy Environ. Sci.*, 2013, **6**, 3483-3507.

- 38 J. L. Xie, C. X. Guo and C. M. Li, *Energy Environ. Sci.*, 2014.
- 39 D. Q. Wu, F. Zhang, H. W. Liang and X. L. Feng, *Chem. Soc. Rev.*, 2012, **41**, 6160-6177.
- 40 V. Chabot, D. Higgins, A. P. Yu, X. C. Xiao, Z. W. Chen and J. J. Zhang, *Energy Environ. Sci.*, 2014, **7**, 1564-1596.
- 41 Z. S. Wu, G. M. Zhou, L. C. Yin, W. Ren, F. Li and H. M. Cheng, *Nano Energy*, 2012, **1**, 107-131.
- 42 L. B. Chen, M. Zhang and W. F. Wei, *J. Nanomater.*, 2013.
- 43 W. Sun and Y. Wang, *Nanoscale*, 2014, **6**, 11528-11552.
- 44 N. Mahmood, C. Zhang, H. Yin and Y. Hou, *J. Mater. Chem. A*, 2014, **2**, 15-32.
- 45 S. Han, D. Wu, S. Li, F. Zhang and X. Feng, *Small*, 2013, 1173-1187.
- 46 H. J. Song, L. C. Zhang, C. L. He, Y. Qu, Y. F. Tian and Y. Lv, *J. Mater. Chem.*, 2011, **21**, 5972-5977.
- 47 J. F. Liang, W. Wei, D. Zhong, Q. L. Yang, L. D. Li and L. Guo, *Acsl Appl. Mater. Inter.*, 2012, **4**, 454-459.
- 48 X. L. Li, W. Qi, D. H. Mei, M. L. Sushko, I. Aksay and J. Liu, *Adv. Mater.*, 2012, **24**, 5136-5141.
- 49 C. Zhong, J. Z. Wang, X. W. Gao, D. Wexler and H. K. Liu, *J. Mater. Chem. A*, 2013, **1**, 10798-10804.
- 50 S. M. Li, B. Wang, J. H. Liu and M. Yu, *Electrochim. Acta*, 2014, **129**, 33-39.
- 51 S. K. Park, A. Jin, S. H. Yu, J. Ha, B. Jang, S. Bong, S. Woo, Y. E. Sung and Y. Piao, *Electrochim. Acta*, 2014, **120**, 452-459.
- 52 B. C. Qiu, M. Y. Xing and J. L. Zhang, *J. Am. Chem. Soc.*, 2014, **136**, 5852-5855.
- 53 D. F. Qiu, G. Bu, B. Zhao, Z. X. Lin, L. Pu, L. J. Pan and Y. Shi, *Mater. Lett.*, 2014, **119**, 12-15.
- 54 S. H. Yu, D. E. Conte, S. Baek, D. C. Lee, S. K. Park, K. J. Lee, Y. Piao, Y. E. Sung and N. Pinna, *Adv. Funct. Mater.*, 2013, **23**, 4293-4305.
- 55 Z. Y. Lu, J. X. Zhu, D. Sim, W. H. Shi, Y. Y. Tay, J. Ma, H. H. Hng and Q. Y. Yan, *Electrochim. Acta*, 2012, **74**, 176-181.
- 56 F. Zou, X. L. Hu, Y. M. Sun, W. Luo, F. F. Xia, L. Qie, Y. Jiang and Y. H. Huang, *Chem-Eur. J.*, 2013, **19**, 6027-6033.
- 57 C. H. Xu, J. Sun and L. Gao, *J. Mater. Chem.*, 2012, **22**, 975-979.
- 58 K. Chang and W. X. Chen, *Chem. Commun.*, 2011, **47**, 4252-4254.
- 59 Z. F. Jiang, C. Wang, G. H. Du, Y. J. Zhong and J. Z. Jiang, *J. Mater. Chem.*, 2012, **22**, 9494-9496.
- 60 H. D. Liu, J. M. Huang, C. J. Xiang, J. Liu and X. L. Li, *J. Mater. Sci.: Mater. El.*, 2013, **24**, 3640-3645.
- 61 L. Noerochim, J. Z. Wang, D. Wexler, Z. Chao and H. K. Liu, *J. Power Sources*, 2013, **228**, 198-205.
- 62 Y. Shi, S. L. Chou, J. Z. Wang, H. J. Li, H. K. Liu and Y. P. Wu, *J. Power Sources*, 2013, **244**, 684-689.
- 63 X. N. Chi, L. Chang, D. Xie, J. Zhang and G. H. Du, *Mater. Lett.*, 2013, **106**, 178-181.
- 64 X. F. Yang, C. Y. Lu, J. L. Qin, R. X. Zhang, H. Tang and H. J. Song, *Mater. Lett.*, 2011, **65**, 2341-2344.
- 65 L. H. Zhuo, Y. Q. Wu, L. Y. Wang, Y. C. Yu, X. B. Zhang and F. Y. Zhao, *Rsc Adv.*, 2012, **2**, 5084-5087.
- 66 G. C. Huang, T. Chen, W. X. Chen, Z. Wang, K. Chang, L. Ma, F. H. Huang, D. Y. Chen and J. Y. Lee, *Small*, 2013, **9**, 3693-3703.
- 67 Y. Zhang, W. C. Wang, P. H. Li, Y. B. Fu and X. H. Ma, *J. Power Sources*, 2012, **210**, 47-53.
- 68 D. N. Wang, X. F. Li, J. J. Wang, J. L. Yang, D. S. Geng, R. Y. Li, M. Cai, T. K. Sham and X. L. Sun, *J. Phys. Chem. C*, 2012, **116**, 22149-22156.
- 69 Y. Chen, B. H. Song, X. S. Tang, L. Lu and J. M. Xue, *J. Mater. Chem.*, 2012, **22**, 17656-17662.
- 70 S. B. Yang, Y. J. Gong, Z. Liu, L. Zhan, D. P. Hashim, L. L. Ma, R. Vajtai and P. M. Ajayan, *Nano Lett.*, 2013, **13**, 1596-1601.
- 71 J. J. Ma, J. L. Wang, Y. S. He, X. Z. Liao, J. Chen, J. Z. Wang, T. Yuan and Z. F. Ma, *J. Mater. Chem. A*, 2014, **2**, 9200-9207.
- 72 N. Li, G. Liu, C. Zhen, F. Li, L. L. Zhang and H. M. Cheng, *Adv. Funct. Mater.*, 2011, **21**, 1717-1722.
- 73 S. Yang, W. B. Yue, J. Zhu, Y. Ren and X. J. Yang, *Adv. Funct. Mater.*, 2013, **23**, 3570-3576.
- 74 R. W. Mo, Z. Y. Lei, K. N. Sun and D. Rooney, *Adv. Mater.*, 2014, **26**, 2084-2088.
- 75 S. Q. Chen, P. Chen and Y. Wang, *Nanoscale*, 2011, **3**, 4323-4329.
- 76 X. F. Li, X. B. Meng, J. Liu, D. S. Geng, Y. Zhang, M. N. Banis, Y. L. Li, J. L. Yang, R. Y. Li, X. L. Sun, M. Cai and M. W. Verbrugge, *Adv. Funct. Mater.*, 2012, **22**, 1647-1654.

- 77 Z. J. Fan, J. Yan, T. Wei, G. Q. Ning, L. J. Zhi, J. C. Liu, D. X. Cao, G. L. Wang and F. Wei, *ACS Nano*, 2011, **5**, 2787-2794.
- 78 K. Evanoff, A. Magasinski, J. B. Yang and G. Yushin, *Adv. Energy Mater.*, 2011, **1**, 495-498.
- 79 W. Li, F. Wang, S. S. Feng, J. X. Wang, Z. K. Sun, B. Li, Y. H. Li, J. P. Yang, A. A. Elzatahry,  
5 Y. Y. Xia and D. Y. Zhao, *J. Am. Chem. Soc.*, 2013, **135**, 18300-18303.
- 80 X. J. Zhu, Y. W. Zhu, S. Murali, M. D. Stollers and R. S. Ruoff, *ACS Nano*, 2011, **5**, 3333-3338.
- 81 X. H. Cao, B. Zheng, X. H. Rui, W. H. Shi, Q. Y. Yan and H. Zhang, *Angew. Chem. Int. Ed.*,  
10 2014, **53**, 1404-1409.
- 82 G. M. Zhou, D. W. Wang, F. Li, L. L. Zhang, N. Li, Z. S. Wu, L. Wen, G. Q. Lu and H. M.  
10 Cheng, *Chem. Mater.*, 2010, **22**, 5306-5313.
- 83 M. Zhang, D. N. Lei, X. M. Yin, L. B. Chen, Q. H. Li, Y. G. Wang and T. H. Wang, *J. Mater. Chem.*, 2010, **20**, 5538-5543.
- 84 Z. S. Wu, W. C. Ren, L. Wen, L. B. Gao, J. P. Zhao, Z. P. Chen, G. M. Zhou, F. Li and H. M.  
Cheng, *ACS Nano*, 2010, **4**, 3187-3194.
- 15 85 S. B. Yang, X. L. Feng, L. Wang, K. Tang, J. Maier and K. Mullen, *Angew. Chem. Int. Ed.*, 2010,  
**49**, 4795-4799.
- 86 X. Xin, X. F. Zhou, J. H. Wu, X. Y. Yao and Z. P. Liu, *ACS Nano*, 2012, **6**, 11035-11043.
- 87 Y. Q. Zou and Y. Wang, *ACS Nano*, 2011, **5**, 8108-8114.
- 88 B. Luo, B. Wang, X. Li, Y. Jia, M. Liang and L. Zhi, *Adv. Mater.*, 2012, **24**, 3538-3543.
- 20 89 B. Luo, B. Wang, M. Liang, J. Ning, X. Li and L. Zhi, *Adv. Mater.*, 2012, **24**, 1405-1409.
- 90 B. Luo, Y. Fang, B. Wang, J. Zhou, H. Song and L. Zhi, *Energy Environ. Sci.*, 2012, **5**, 5226-  
5230.
- 91 P. Wu, H. Wang, Y. W. Tang, Y. M. Zhou and T. H. Lu, *Acs Appl. Mater. Inter.*, 2014, **6**, 3546-  
3552.
- 25 92 X. H. Rui, J. X. Zhu, D. Sim, C. Xu, Y. Zeng, H. H. Hng, T. M. Lim and Q. Y. Yan, *Nanoscale*,  
2011, **3**, 4752-4758.
- 93 K. J. Zhang, H. B. Wang, X. Q. He, Z. H. Liu, L. Wang, L. Gu, H. X. Xu, P. X. Han, S. M. Dong,  
C. J. Zhang, J. H. Yao, G. L. Cui and L. Q. Chen, *J. Mater. Chem.*, 2011, **21**, 11916-11922.
- 94 H. L. Wang, Y. Yang, Y. Y. Liang, L. F. Cui, H. S. Casalongue, Y. G. Li, G. S. Hong, Y. Cui and  
30 H. J. Dai, *Angew. Chem. Int. Ed.*, 2011, **50**, 7364-7368.
- 95 Y. Tang, F. Huang, W. Zhao, Z. Liu and D. Wan, *J. Mater. Chem.*, 2012, **22**, 11257-11260.
- 96 Z. Y. Sun, K. P. Xie, Z. A. Li, I. Sinev, P. Ebbinghaus, A. Erbe, M. Farle, W. Schuhmann, M.  
Muhler and E. Ventosa, *Chem-Eur. J.*, 2014, **20**, 2022-2030.
- 97 A. Chidembo, S. H. Aboutalebi, K. Konstantinov, M. Salari, B. Winton, S. A. Yamini, I. P.  
35 Nevirkovets and H. K. Liu, *Energy Environ. Sci.*, 2012, **5**, 5236-5240.
- 98 C. X. Peng, B. D. Chen, Y. Qin, S. H. Yang, C. Z. Li, Y. H. Zuo, S. Y. Liu and J. H. Yang, *ACS Nano*,  
2012, **6**, 1074-1081.
- 99 H. Kim, Y. Son, C. Park, J. Cho and H. C. Choi, *Angew. Chem. Int. Ed.*, 2013, **52**, 5997-6001.
- 100 C. Wang, J. Ju, Y. Q. Yang, Y. F. Tang, J. H. Lin, Z. J. Shi, R. P. S. Han and F. Q. Huang, *J.  
40 Mater. Chem. A*, 2013, **1**, 8897-8902.
- 101 B. Wang, X. Li, X. Zhang, B. Luo, M. Jin, M. Liang, S. A. Dayeh, S. T. Picraux and L. Zhi,  
*ACS Nano*, 2013, **7**, 1437-1445.
- 102 B. Wang, X. Li, X. Zhang, B. Luo, Y. Zhang and L. Zhi, *Adv. Mater.*, 2013, **25**, 3560-3565.
- 103 B. Wang, X. Li, T. Qiu, B. Luo, J. Ning, J. Li, X. Zhang, M. Liang and L. Zhi, *Nano Lett.*, 2013,  
45 **13**, 5578-5584.
- 104 Z. X. Chen, M. Zhou, Y. L. Cao, X. P. Ai, H. X. Yang and J. Liu, *Adv. Energy Mater.*, 2012, **2**,  
95-102.
- 105 V. Etacheri, J. E. Yourey and B. M. Bartlett, *ACS Nano*, 2014, **8**, 1491-1499.
- 106 H. Bai, C. Li and G. Q. Shi, *Adv. Mater.*, 2011, **23**, 1089-1115.
- 50 107 W. F. Chen, S. R. Li, C. H. Chen and L. F. Yan, *Adv. Mater.*, 2011, **23**, 5679-5683.
- 108 G. Zhu, Y. Liu, Z. Xu, T. Jiang, C. Zhang, X. Li and G. Qi, *ChemPhysChem*, 2010, **11**, 2432-  
2437.
- 109 S. B. Yang, X. L. Feng, S. Ivanovici and K. Mullen, *Angew. Chem. Int. Ed.*, 2010, **49**, 8408-  
8411.
- 55 110 S. Chabi, C. Peng, D. Hu and Y. Q. Zhu, *Adv. Mater.*, 2014, **26**, 2440-2445.
- 111 R. Liu, J. Duay and S. B. Lee, *Chem. Commun.*, 2011, **47**, 1384-1404.
- 112 Q. F. Zhang, E. Uchaker, S. L. Candelaria and G. Z. Cao, *Chem. Soc. Rev.*, 2013, **42**, 3127-  
3171.
- 113 A. S. Arico, P. Bruce, B. Scrosati, J. M. Tarascon and W. Van Schalkwijk, *Nat. Mater.*, 2005, **4**,  
60 366-377.
- 114 B. Wang, B. Luo, X. Li and L. Zhi, *Mater. Today*, 2012, **15**, 544-552.

- 115 L. W. Ji, Z. Lin, M. Alcoutlabi and X. W. Zhang, *Energy Environ. Sci.*, 2011, **4**, 2682-2699.  
116 X. L. Li and L. J. Zhi, *Nanoscale*, 2013, **5**, 8864-8873.  
117 S. M. Paek, E. Yoo and I. Honma, *Nano Lett.*, 2009, **9**, 72-75.  
118 R. L. Liang, H. Q. Cao, D. Qian, J. X. Zhang and M. Z. Qu, *J. Mater. Chem.*, 2011, **21**, 17654-  
5 17657.  
119 H. Kim, S. W. Kim, Y. U. Park, H. Gwon, D. H. Seo, Y. Kim and K. Kang, *Nano Res.*, 2010, **3**,  
813-821.  
120 D. H. Wang, R. Kou, D. Choi, Z. G. Yang, Z. M. Nie, J. Li, L. V. Saraf, D. H. Hu, J. G. Zhang,  
G. L. Graff, J. Liu, M. A. Pope and I. A. Aksay, *ACS Nano*, 2010, **4**, 1587-1595.  
10 121 X. S. Zhou, Y. X. Yin, L. J. Wan and Y. G. Guo, *J. Mater. Chem.*, 2012, **22**, 17456-17459.  
122 Y. Z. Su, S. Li, D. Q. Wu, F. Zhang, H. W. Liang, P. F. Gao, C. Cheng and X. L. Feng, *ACS  
Nano*, 2012, **6**, 8349-8356.  
123 B. J. Li, H. Q. Cao, J. X. Zhang, M. Z. Qu, F. Lian and X. H. Kong, *J. Mater. Chem.*, 2012, **22**,  
2851-2854.  
15 124 Y. Li, S. M. Zhu, Q. L. Liu, J. J. Gu, Z. P. Guo, Z. X. Chen, C. L. Feng, D. Zhang and W. J.  
Moon, *J. Mater. Chem.*, 2012, **22**, 2766-2773.  
125 J. J. Tang, J. Yang, L. M. Zhou, J. Xie, G. H. Chen and X. Y. Zhou, *J. Mater. Chem. A*, 2014, **2**,  
6292-6295.  
126 L. S. Zhang, L. Y. Jiang, H. J. Yan, W. D. Wang, W. Wang, W. G. Song, Y. G. Guo and L. J.  
20 Wan, *J. Mater. Chem.*, 2010, **20**, 5462-5467.  
127 R. H. Wang, C. H. Xu, J. Sun, L. Gao and H. L. Yao, *Acs Appl. Mater. Inter.*, 2014, **6**, 3427-  
3436.  
128 J. Lin, Z. W. Peng, C. S. Xiang, G. D. Ruan, Z. Yan, D. Natelson and J. M. Tour, *ACS Nano*,  
2013, **7**, 6001-6006.  
25 129 S. Mao, Z. H. Wen, H. Kim, G. H. Lu, P. Hurley and J. H. Chen, *ACS Nano*, 2012, **6**, 7505-  
7513.  
130 Y. S. Huang, D. Q. Wu, S. Han, S. Li, L. Xiao, F. Zhang and X. L. Feng, *Chemsuschem*, 2013,  
**6**, 1510-1515.  
131 Z. T. Li, G. L. Wu, D. Liu, W. T. Wu, B. Jiang, J. T. Zheng, Y. P. Li, J. H. Li and M. B. Wu, *J.  
Mater. Chem. A*, 2014, **2**, 7471-7477.  
132 H. W. Song, N. Li, H. Cui and C. X. Wang, *J. Mater. Chem. A*, 2013, **1**, 7558-7562.  
133 Y. M. Li, X. J. Lv, J. Lu and J. H. Li, *J. Phys. Chem. C*, 2010, **114**, 21770-21774.  
134 Q. Guo, S. S. Chen and X. Qin, *Mater. Lett.*, 2014, **119**, 4-7.  
135 H. Kim, D. H. Seo, S. W. Kim, J. Kim and K. Kang, *Carbon*, 2011, **49**, 326-332.  
35 136 B. G. Choi, S. J. Chang, Y. B. Lee, J. S. Bae, H. J. Kim and Y. S. Huh, *Nanoscale*, 2012, **4**,  
5924-5930.  
137 S. B. Yang, G. L. Cui, S. P. Pang, Q. Cao, U. Kolb, X. L. Feng, J. Maier and K. Mullen,  
*Chemsuschem*, 2010, **3**, 236-239.  
138 X. L. Yang, K. C. Fan, Y. H. Zhu, J. H. Shen, X. Jiang, P. Zhao and C. Z. Li, *J. Mater. Chem.*,  
40 2012, **22**, 17278-17283.  
139 A. K. Rai, J. Gim, L. T. Anh and J. Kim, *Electrochim. Acta*, 2013, **100**, 63-71.  
140 B. J. Li, H. Q. Cao, J. Shao, G. Q. Li, M. Z. Qu and G. Yin, *Inorg. Chem.*, 2011, **50**, 1628-1632.  
141 J. Z. Wang, C. Zhong, D. Wexler, N. H. Idris, Z. X. Wang, L. Q. Chen and H. K. Liu, *Chem-  
Eur. J.*, 2011, **17**, 661-667.  
45 142 L. W. Ji, Z. K. Tan, T. R. Kuykendall, S. Aloni, S. D. Xun, E. Lin, V. Battaglia and Y. G.  
Zhang, *Phys. Chem. Chem. Phys.*, 2011, **13**, 7139-7146.  
143 D. Y. Chen, G. Ji, Y. Ma, J. Y. Lee and J. M. Lu, *Acs Appl. Mater. Inter.*, 2011, **3**, 3078-3083.  
144 B. J. Li, H. Q. Cao, J. Shao and M. Z. Qu, *Chem. Commun.*, 2011, **47**, 10374-10376.  
145 B. J. Li, H. Q. Cao, J. Shao, M. Z. Qu and J. H. Warner, *J. Mater. Chem.*, 2011, **21**, 5069-5075.  
50 146 C. T. Hsieh, J. Y. Lin and C. Y. Mo, *Electrochim. Acta*, 2011, **58**, 119-124.  
147 C. L. Liang, T. Zhai, W. Wang, J. Chen, W. X. Zhao, X. H. Lu and Y. X. Tong, *J. Mater. Chem.  
A*, 2014, **2**, 7214-7220.  
148 Y. Q. Zou, J. Kan and Y. Wang, *J. Phys. Chem. C*, 2011, **115**, 20747-20753.  
149 M. Zhang, B. H. Qu, D. N. Lei, Y. J. Chen, X. Z. Yu, L. B. Chen, Q. H. Li, Y. G. Wang and T.  
55 H. Wang, *J. Mater. Chem.*, 2012, **22**, 3868-3874.  
150 S. Bai, S. Q. Chen, X. P. Shen, G. X. Zhu and G. X. Wang, *Rsc Adv.*, 2012, **2**, 10977-10984.  
151 X. Zhu, X. Y. Song, X. L. Ma and G. Q. Ning, *Acs Appl. Mater. Inter.*, 2014, **6**, 7189-7197.  
152 J. Lin, A. R. O. Raji, K. W. Nan, Z. W. Peng, Z. Yan, E. L. G. Samuel, D. Natelson and J. M.  
Tour, *Adv. Funct. Mater.*, 2014, **24**, 2044-2048.  
60 153 Z. L. Jian, B. Zhao, P. Liu, F. J. Li, M. B. Zheng, M. W. Chen, Y. Shi and H. S. Zhou, *Chem.  
Commun.*, 2014, **50**, 1215-1217.

- 154 O. Vargas, A. Caballero and J. Morales, *Electrochim. Acta*, 2014, **130**, 551-558.
- 155 J. Ye, J. Zhang, F. X. Wang, Q. M. Su and G. H. Du, *Electrochim. Acta*, 2013, **113**, 212-217.
- 156 H. L. Wang, L. F. Cui, Y. A. Yang, H. S. Casalongue, J. T. Robinson, Y. Y. Liang, Y. Cui and H. J. Dai, *J. Am. Chem. Soc.*, 2010, **132**, 13978-13980.
- 5 157 X. Zhao, C. M. Hayner and H. H. Kung, *J. Mater. Chem.*, 2011, **21**, 17297-17303.
- 158 L. Li, Z. Guo, A. Du and H. Liu, *J. Mater. Chem.*, 2012, **22**, 3600-3605.
- 159 S. Y. Liu, J. Xie, Y. X. Zheng, G. S. Cao, T. J. Zhu and X. B. Zhao, *Electrochim. Acta*, 2012, **66**, 271-278.
- 160 C. X. Guo, M. Wang, T. Chen, X. W. Lou and C. M. Li, *Adv. Energy Mater.*, 2011, **1**, 736-741.
- 10 161 Y. Y. Li, Q. W. Zhang, J. L. Zhu, X. L. Wei and P. K. Shen, *J. Mater. Chem. A*, 2014, **2**, 3163-3168.
- 162 S. H. Choi and Y. C. Kang, *Chemsuschem*, 2014, **7**, 523-528.
- 163 K. H. Seng, G. D. Du, L. Li, Z. X. Chen, H. K. Liu and Z. P. Guo, *J. Mater. Chem.*, 2012, **22**, 16072-16077.
- 15 164 F. Xia, X. Hu, Y. Sun, W. Luo and Y. Huang, *Nanoscale*, 2012, **4**, 4707-4711.
- 165 Y. M. Sun, X. L. Hu, W. Luo and Y. H. Huang, *ACS Nano*, 2011, **5**, 7100-7107.
- 166 Y. J. Mai, X. L. Wang, J. Y. Xiang, Y. Q. Qiao, D. Zhang, C. D. Gu and J. P. Tu, *Electrochim. Acta*, 2011, **56**, 2306-2311.
- 167 L. Q. Tao, J. T. Zai, K. X. Wang, Y. H. Wan, H. J. Zhang, C. Yu, Y. L. Xiao and X. F. Qian, *Rsc Adv.*, 2012, **2**, 3410-3415.
- 168 Y. J. Mai, J. P. Tu, C. D. Gu and X. L. Wang, *J. Power Sources*, 2012, **209**, 1-6.
- 169 I. R. M. Kottegoda, N. H. Idris, L. Lu, J. Z. Wang and H. K. Liu, *Electrochim. Acta*, 2011, **56**, 5815-5822.
- 170 C. T. Hsieh, C. Y. Lin, Y. F. Chen and J. S. Lin, *Electrochim. Acta*, 2013, **111**, 359-365.
- 25 171 H. Q. Cao, B. J. Li, J. X. Zhang, F. Lian, X. H. Kong and M. Z. Qu, *J. Mater. Chem.*, 2012, **22**, 9759-9766.
- 172 J. X. Qiu, P. Zhang, M. Ling, S. Li, P. R. Liu, H. J. Zhao and S. Q. Zhang, *Acs Appl. Mater. Inter.*, 2012, **4**, 3636-3642.
- 173 J. S. Chen, Z. Y. Wang, X. C. Dong, P. Chen and X. W. Lou, *Nanoscale*, 2011, **3**, 2158-2161.
- 30 174 D. H. Wang, D. W. Choi, J. Li, Z. G. Yang, Z. M. Nie, R. Kou, D. H. Hu, C. M. Wang, L. V. Saraf, J. G. Zhang, I. A. Aksay and J. Liu, *ACS Nano*, 2009, **3**, 907-914.
- 175 G. X. Wang, B. Wang, X. L. Wang, J. Park, S. X. Dou, H. Ahn and K. Kim, *J. Mater. Chem.*, 2009, **19**, 8378-8384.
- 176 S. Q. Chen, P. Chen, M. H. Wu, D. Y. Pan and Y. Wang, *Electrochim. Commun.*, 2010, **12**, 1302-1306.
- 35 177 J. Qin, C. N. He, N. Q. Zhao, Z. Y. Wang, C. S. Shi, E. Z. Liu and J. J. Li, *ACS Nano*, 2014, **8**, 1728-1738.
- 178 S. N. Yang, G. R. Li, Q. Zhu and Q. M. Pan, *J. Mater. Chem.*, 2012, **22**, 3420-3425.
- 179 J. Z. Wang, C. Zhong, S. L. Chou and H. K. Liu, *Electrochim. Commun.*, 2010, **12**, 1467-1470.
- 40 180 J. Y. Luo, X. Zhao, J. S. Wu, H. D. Jang, H. H. Kung and J. X. Huang, *J. Phys. Chem. Lett.*, 2012, **3**, 1824-1829.
- 181 X. Zhao, C. M. Hayner, M. C. Kung and H. H. Kung, *Adv. Energy Mater.*, 2011, **1**, 1079-1084.
- 182 X. Xin, X. F. Zhou, F. Wang, X. Y. Yao, X. X. Xu, Y. M. Zhu and Z. P. Liu, *J. Mater. Chem.*, 2012, **22**, 7724-7730.
- 45 183 J. K. Lee, K. B. Smith, C. M. Hayner and H. H. Kung, *Chem. Commun.*, 2010, **46**, 2025-2027.
- 184 Y. Wen, Y. J. Zhu, A. Langrock, A. Manivannan, S. H. Ehrman and C. S. Wang, *Small*, 2013, **9**, 2810-2816.
- 185 H.-C. Tao, L.-Z. Fan, Y. Mei and X. Qu, *Electrochim. Commun.*, 2011, **13**, 1332-1335.
- 186 X. Zhou, Y.-X. Yin, L.-J. Wan and Y.-G. Guo, *Adv. Energy Mater.*, 2012, **2**, 1086-1090.
- 50 187 X. Zhou, Y.-X. Yin, L.-J. Wan and Y.-G. Guo, *Chem. Commun.*, 2012, **48**, 2198-2200.
- 188 Z. F. Li, H. Y. Zhang, Q. Liu, Y. D. Liu, L. Stanciu and J. Xie, *Acs Appl. Mater. Inter.*, 2014, **6**, 5996-6002.
- 189 C. Chae, H. J. Noh, J. K. Lee, B. Scrosati and Y. K. Sun, *Adv. Funct. Mater.*, 2014, **24**, 3036-3042.
- 55 190 C. L. Ma, C. Ma, J. Z. Wang, H. Q. Wang, J. L. Shi, Y. Song, Q. G. Guo and L. Liu, *Carbon*, 2014, **72**, 38-46.
- 191 D. P. Wong, H. P. Tseng, Y. T. Chen, B. J. Hwang, L. C. Chen and K. H. Chen, *Carbon*, 2013, **63**, 397-403.
- 60 192 H. F. Xiang, K. Zhang, G. Ji, J. Y. Lee, C. J. Zou, X. D. Chen and J. S. Wu, *Carbon*, 2011, **49**, 1787-1796.

- 193 L. Zhang, W. W. Hao, H. B. Wang, L. F. Zhang, X. M. Feng, Y. B. Zhang, W. X. Chen, H. Pang and H. H. Zheng, *J. Mater. Chem. A*, 2013, **1**, 7601-7611.
- 194 F. Sun, K. Huang, X. Qi, T. Gao, Y. P. Liu, X. H. Zou, X. L. Wei and J. X. Zhong, *Nanoscale*, 2013, **5**, 8586-8592.
- 195 J. S. Cheng and J. Du, *Crystengcomm*, 2012, **14**, 397-400.
- 196 J. G. Ren, Q. H. Wu, H. Tang, G. Hong, W. J. Zhang and S. T. Lee, *J. Mater. Chem. A*, 2013, **1**, 1821-1826.
- 197 D.-J. Xue, S. Xin, Y. Yan, K.-C. Jiang, Y.-X. Yin, Y.-G. Guo and L.-J. Wan, *J. Am. Chem. Soc.*, 2012, **134**, 2512-2515.
- 198 F. W. Yuan and H. Y. Tuan, *Chem. Mater.*, 2014, **26**, 2172-2179.
- 199 D. P. Lv, M. L. Gordin, R. Yi, T. Xu, J. X. Song, Y. B. Jiang, D. Choi and D. H. Wang, *Adv. Funct. Mater.*, 2014, **24**, 1059-1066.
- 200 S. G. Ri, L. Zhan, Y. Wang, L. H. Zhou, J. Hu and H. L. Liu, *Electrochim. Acta*, 2013, **109**, 389-394.
- 201 H. Xia, D. D. Zhu, Y. S. Fu and X. Wang, *Electrochim. Acta*, 2012, **83**, 166-174.
- 202 Y. Q. Cao, L. Zhang, D. L. Tao, D. X. Huo and K. P. Su, *Electrochim. Acta*, 2014, **132**, 483-489.
- 203 G. M. Zhou, L. C. Yin, D. W. Wang, L. Li, S. F. Pei, I. R. Gentle, F. Li and H. M. Cheng, *ACS Nano*, 2013, **7**, 5367-5375.
- 204 T. Q. Lin, Y. F. Tang, Y. M. Wang, H. Bi, Z. Q. Liu, F. Q. Huang, X. M. Xie and M. H. Jiang, *Energy Environ. Sci.*, 2013, **6**, 1283-1290.
- 205 L. C. Yin, J. L. Wang, F. J. Lin, J. Yang and Y. Nuli, *Energy Environ. Sci.*, 2012, **5**, 6966-6972.
- 206 L. W. Ji, M. M. Rao, H. M. Zheng, L. Zhang, Y. C. Li, W. H. Duan, J. H. Guo, E. J. Cairns and Y. G. Zhang, *J. Am. Chem. Soc.*, 2011, **133**, 18522-18525.
- 207 H. L. Wang, Y. Yang, Y. Y. Liang, J. T. Robinson, Y. G. Li, A. Jackson, Y. Cui and H. J. Dai, *Nano Lett.*, 2011, **11**, 2644-2647.
- 208 H. L. Fei, Z. W. Peng, Y. Yang, L. Li, A. R. O. Raji, E. L. G. Samuel and J. M. Tour, *Chem. Commun.*, 2014, **50**, 7117-7119.
- 209 J. L. Yang, J. J. Wang, Y. J. Tang, D. N. Wang, X. F. Li, Y. H. Hu, R. Y. Li, G. X. Liang, T. K. Sham and X. L. Sun, *Energy Environ. Sci.*, 2013, **6**, 1521-1528.
- 210 Y. Shi, S. L. Chou, J. Z. Wang, D. Wexler, H. J. Li, H. K. Liu and Y. P. Wu, *J. Mater. Chem.*, 2012, **22**, 16465-16470.
- 211 J. Ha, S. K. Park, S. H. Yu, A. Jin, B. Jang, S. Bong, I. Kim, Y. E. Sung and Y. Piao, *Nanoscale*, 2013, **5**, 8647-8655.
- 212 R. W. Mo, Z. Y. Lei, D. Rooney and K. N. Sun, *Electrochim. Acta*, 2014, **130**, 594-599.
- 213 X. Zhao, C. M. Hayner, M. C. Kung and H. H. Kung, *Chem. Commun.*, 2012, **48**, 9909-9911.
- 214 W. W. Zhou, J. X. Zhu, C. W. Cheng, J. P. Liu, H. P. Yang, C. X. Cong, C. Guan, X. T. Jia, H. J. Fan, Q. Y. Yan, C. M. Li and T. Yu, *Energy Environ. Sci.*, 2011, **4**, 4954-4961.
- 215 B. Wang, X. Li, B. Luo, Y. Jia and L. Zhi, *Nanoscale*, 2013, **5**, 1470-1474.
- 216 S. E. Lee, H. J. Kim, H. Kim, J. H. Park and D. G. Choi, *Nanoscale*, 2013, **5**, 8986-8991.
- 217 Y. Yang, J. G. Ren, X. Wang, Y. S. Chui, Q. H. Wu, X. F. Chen and W. J. Zhang, *Nanoscale*, 2013, **5**, 8689-8694.
- 218 J. G. Ren, C. D. Wang, Q. H. Wu, X. Liu, Y. Yang, L. F. He and W. J. Zhang, *Nanoscale*, 2014, **6**, 3353-3360.
- 219 J. Hou, R. Wu, P. J. Zhao, A. M. Chang, G. Ji, B. Gao and Q. Zhao, *Mater. Lett.*, 2013, **100**, 173-176.
- 220 H. M. Liu and W. S. Yang, *Energy Environ. Sci.*, 2011, **4**, 4000-4008.
- 221 J. W. Lee, S. Y. Lim, H. M. Jeong, T. H. Hwang, J. K. Kang and J. W. Choi, *Energy Environ. Sci.*, 2012, **5**, 9889-9894.
- 222 Y. Q. Qian, A. Vu, W. Smyrl and A. Stein, *J. Electrochem. Soci.*, 2012, **159**, A1135-A1140.
- 223 L. Y. Liang, Y. M. Xu, Y. Lei and H. M. Liu, *Nanoscale*, 2014, **6**, 3536-3539.
- 224 L. W. Ji, Z. K. Tan, T. Kuykendall, E. J. An, Y. B. Fu, V. Battaglia and Y. G. Zhang, *Energy Environ. Sci.*, 2011, **4**, 3611-3616.
- 225 H. D. Liu, J. M. Huang, X. L. Li, J. Liu and Y. X. Zhang, *Ceram. Int.*, 2012, **38**, 5145-5149.
- 226 C. H. Xu, J. Sun and L. Gao, *Nanoscale*, 2012, **4**, 5425-5430.
- 227 S. M. Jiang, B. T. Zhao, R. Ran, R. Cai, M. O. Tade and Z. P. Shao, *Rsc Adv.*, 2014, **4**, 9367-9371.
- 228 A. P. Hu, X. H. Chen, Y. H. Tang, Q. L. Tang, L. Yang and S. P. Zhang, *Electrochim. Commun.*, 2013, **28**, 139-142.
- 229 X. L. Yang, K. C. Fan, Y. H. Zhu, J. H. Shen, X. Jiang, P. Zhao, S. R. Luan and C. Z. Li, *Ac. Appl. Mater. Inter.*, 2013, **5**, 997-1002.

- 230 F. Y. Tu, T. H. Wu, S. Q. Liu, G. H. Jin and C. Y. Pan, *Electrochim. Acta*, 2013, **106**, 406-410.
- 231 Y. Yu, B. Zhang, Y. B. He, Z. D. Huang, S. W. Oh and J. K. Kim, *J. Mater. Chem. A*, 2013, **1**, 1163-1170.
- 232 L. Li, A. R. O. Raji and J. M. Tour, *Adv. Mater.*, 2013, **25**, 6298-6302.
- 233 Y. Liu, W. Wang, Y. W. Wang, Y. L. Ying, L. W. Sun and X. S. Peng, *Rsc Adv.*, 2014, **4**, 16374-16379.
- 234 Z. M. Zheng, Y. L. Cheng, X. B. Yan, R. T. Wang and P. Zhang, *J. Mater. Chem. A*, 2014, **2**, 149-154.
- 235 S. H. Lee, V. Sridhar, J. H. Jung, K. Karthikeyan, Y. S. Lee, R. Mukherjee, N. Koratkar and I. K. Oh, *ACS Nano*, 2013, **7**, 4242-4251.
- 236 J. Wang, Y. K. Zhou, B. Xiong, Y. Y. Zhao, X. J. Huang and Z. P. Shao, *Electrochim. Acta*, 2013, **88**, 847-857.
- 237 Y. Long, Y. Shu, X. H. Ma and M. X. Ye, *Electrochim. Acta*, 2014, **117**, 105-112.
- 238 M. S. Xu, T. Liang, M. M. Shi and H. Z. Chen, *Chem. Rev.*, 2013, **113**, 3766-3798.
- 239 C. N. R. Rao, H. Matte and U. Maitra, *Angew. Chem. Int. Ed.*, 2013, **52**, 13162-13185.
- 240 H. Li, J. Wu, Z. Yin and H. Zhang, *Accounts Chem. Res.*, 2014, **47**, 1067-1075.
- 241 X. Huang, Z. Zeng and H. Zhang, *Chem. Soc. Rev.*, 2013, **42**, 1934-1946.
- 242 M. Chhowalla, H. S. Shin, G. Eda, L.-J. Li, K. P. Loh and H. Zhang, *Nat Chem*, 2013, **5**, 263-275.
- 243 A. Castellanos-Gomez, M. Poot, G. A. Steele, H. S. J. van der Zant, N. Agrait and G. Rubio-Bollinger, *Adv. Mater.*, 2012, **24**, 772-775.
- 244 J.-W. Seo, Y.-W. Jun, S.-W. Park, H. Nah, T. Moon, B. Park, J.-G. Kim, Y. J. Kim and J. Cheon, *Angew. Chem. Int. Ed.*, 2007, **46**, 8828-8831.
- 245 Z. Zeng, Z. Yin, X. Huang, H. Li, Q. He, G. Lu, F. Boey and H. Zhang, *Angew. Chem. Int. Ed.*, 2011, **50**, 11093-11097.
- 246 H. Hwang, H. Kim and J. Cho, *Nano Lett.*, 2011, **11**, 4826-4830.
- 247 D. Golberg, *Nat. Nanotechnol.*, 2011, **6**, 200-201.
- 248 B. Radisavljevic, A. Radenovic, J. Brivio, V. Giacometti and A. Kis, *Nat. Nanotechnol.*, 2011, **6**, 147-150.
- 249 J. N. Coleman, M. Lotya, A. O'Neill, S. D. Bergin, P. J. King, U. Khan, K. Young, A. Gaucher, S. De, R. J. Smith, I. V. Shvets, S. K. Arora, G. Stanton, H.-Y. Kim, K. Lee, G. T. Kim, G. S. Duesberg, T. Hallam, J. J. Boland, J. J. Wang, J. F. Donegan, J. C. Grunlan, G. Moriarty, A. Shmeliov, R. J. Nicholls, J. M. Perkins, E. M. Grieveson, K. Theuwissen, D. W. McComb, P. D. Nellist and V. Nicolosi, *Science*, 2011, **331**, 568-571.
- 250 X. Huang, C. Tan, Z. Yin and H. Zhang, *Adv. Mater.*, 2014, **26**, 2185-2204.
- 251 J. Liu, Z. Zeng, X. Cao, G. Lu, L.-H. Wang, Q.-L. Fan, W. Huang and H. Zhang, *Small*, 2012, **8**, 3517-3522.
- 252 H. Li, Z. Yin, Q. He, H. Li, X. Huang, G. Lu, D. W. H. Fam, A. I. Y. Tok, Q. Zhang and H. Zhang, *Small*, 2012, **8**, 63-67.
- 253 X. Huang, Z. Zeng, Z. Fan, J. Liu and H. Zhang, *Adv. Mater.*, 2012, **24**, 5979-6004.
- 254 W. Zhou, X. Cao, Z. Zeng, W. Shi, Y. Zhu, Q. Yan, H. Liu, J. Wang and H. Zhang, *Energy Environ. Sci.*, 2013, **6**, 2216-2221.
- 255 K. Chang and W. Chen, *ACS Nano*, 2011, **5**, 4720-4728.
- 256 P. V. Prikhodchenko, J. Gun, S. Sladkevich, A. A. Mikhaylov, O. Lev, Y. Y. Tay, S. K. Batabyal and D. Y. W. Yu, *Chem. Mater.*, 2012, **24**, 4750-4757.
- 257 F. Ye, G. Du, Z. Jiang, Y. Zhong, X. Wang, Q. Cao and J. Z. Jiang, *Nanoscale*, 2012, **4**, 7354-7357.
- 258 K. Chang and W. Chen, *J. Mater. Chem.*, 2011, **21**, 17175-17184.
- 259 Y. Li, H. Wang, L. Xie, Y. Liang, G. Hong and H. Dai, *J. Am. Chem. Soc.*, 2011, **133**, 7296-7299.
- 260 Q. Xiang, J. Yu and M. Jaroniec, *J. Am. Chem. Soc.*, 2012, **134**, 6575-6578.
- 261 J. F. Yin, H. Q. Cao, Z. F. Zhou, J. X. Zhang and M. Z. Qu, *J. Mater. Chem.*, 2012, **22**, 23963-23970.
- 262 K. Chang, D. S. Geng, X. F. Li, J. L. Yang, Y. J. Tang, M. Cai, R. Y. Li and X. L. Sun, *Adv. Energy Mater.*, 2013, **3**, 839-844.
- 263 J. Xiao, X. J. Wang, X. Q. Yang, S. D. Xun, G. Liu, P. K. Koech, J. Liu and J. P. Lemmon, *Adv. Funct. Mater.*, 2011, **21**, 2840-2846.
- 264 Z. Wang, T. Chen, W. X. Chen, K. Chang, L. Ma, G. C. Huang, D. Y. Chen and J. Y. Lee, *J. Mater. Chem. A*, 2013, **1**, 2202-2210.
- 265 Q. F. Wang, Y. Huang, J. Miao, Y. Zhao, W. Zhang and Y. Wang, *J Am Ceram Soc*, 2013, **96**, 2190-2196.

- 266 L. Zhi, D. Kong, H. He, q. song, B. Wang, W. Lv and Q.-H. Yang, *Energy Environ. Sci.*, 2014.
- 267 A. Garcia-Gallastegui, D. Iruretagoyena, V. Gouvea, M. Mokhtar, A. M. Asiri, S. N. Basahel, S. A. Al-Thabaiti, A. O. Alyoubi, D. Chadwick and M. S. P. Shaffer, *Chem. Mater.*, 2012, **24**, 4531-4539.
- 268 T. Xiao, X. Hu, B. Heng, X. Chen, W. Huang, W. Tao, H. Wang, Y. Tang, X. Tan and X. Huang, *J Alloy Compd.*, 2013, **549**, 147-151.
- 269 Y. S. He, D. W. Bai, X. W. Yang, J. Chen, X. Z. Liao and Z. F. Ma, *Electrochim. Commun.*, 2010, **12**, 570-573.
- 270 X. L. Huang, J. Chai, T. Jiang, Y. J. Wei, G. Chen, W. Q. Liu, D. X. Han, L. Niu, L. M. Wang and X. B. Zhang, *J. Mater. Chem.*, 2012, **22**, 3404-3410.
- 271 S. Ding, D. Luan, F. Y. C. Boey, J. S. Chen and X. W. Lou, *Chem. Commun.*, 2011, **47**, 7155-7157.
- 272 S. J. Ding, J. S. Chen, D. Y. Luan, F. Y. C. Boey, S. Madhavi and X. W. Lou, *Chem. Commun.*, 2011, **47**, 5780-5782.
- 273 H. Zhao, L. Pan, S. Xing, J. Luo and J. Xu, *J. Power Sources*, 2013, **222**, 21-31.
- 274 Y. Q. Zou and Y. Wang, *Nanoscale*, 2011, **3**, 2615-2620.
- 275 J. Qu, Y. X. Yin, Y. Q. Wang, Y. Yan, Y. G. Guo and W. G. Song, *Acs Appl. Mater. Inter.*, 2013, **5**, 3932-3936.
- 276 S. J. Ding, D. Y. Luan, F. Y. C. Boey, J. S. Chen and X. W. Lou, *Chem. Commun.*, 2011, **47**, 7155-7157.
- 277 S. G. Hwang, G. O. Kim, S. R. Yun and K. S. Ryu, *Electrochim. Acta*, 2012, **78**, 406-411.
- 278 Y. Huang, X. L. Huang, J. S. Lian, D. Xu, L. M. Wang and X. B. Zhang, *J. Mater. Chem.*, 2012, **22**, 2844-2847.
- 279 L. Q. Lu and Y. Wang, *J. Mater. Chem.*, 2011, **21**, 17916-17921.
- 280 Z. Y. Wang, J. W. Sha, E. Z. Liu, C. N. He, C. S. Shi, J. J. Li and N. Q. Zhao, *J. Mater. Chem. A*, 2014, **2**, 8893-8901.
- 281 Y. J. Chen, J. Zhu, B. H. Qu, B. A. Lu and Z. Xu, *Nano Energy*, 2014, **3**, 88-94.
- 282 B. Wang, S. Wang, P. Liu, J. Deng, B. H. Xu, T. F. Liu, D. L. Wang and X. S. Zhao, *Mater. Lett.*, 2014, **118**, 137-141.
- 283 M. S. Whittingham, *Chem. Rev.*, 2004, **104**, 4271-4301.
- 284 G. D. Du, Z. P. Guo, S. Q. Wang, R. Zeng, Z. X. Chen and H. K. Liu, *Chem. Commun.*, 2010, **46**, 1106-1108.
- 285 S. Y. Liu, X. Lu, J. Xie, G. S. Cao, T. J. Zhu and X. B. Zhao, *Acs Appl. Mater. Inter.*, 2013, **5**, 1588-1595.
- 286 M. Sathish, S. Mitani, T. Tomai and I. Honma, *J. Phys. Chem. C*, 2012, **116**, 12475-12481.
- 287 K. Chang, Z. Wang, G. C. Huang, H. Li, W. X. Chen and J. Y. Lee, *J. Power Sources*, 2012, **201**, 259-266.
- 288 D. Kong, H. He, Q. Song, B. Wang, Q.-H. Yang and L. Zhi, *Rsc Adv.*, 2014, **4**, 23372-23376.
- 289 J. Choi, J. Jin, J. Lee, J. H. Park, H. J. Kim, D. H. Oh, J. R. Ahn and S. U. Son, *J. Mater. Chem.*, 2012, **22**, 11107-11112.
- 290 Y. Gu, Y. Xu and Y. Wang, *Acs Appl. Mater. Inter.*, 2013, **5**, 801-806.
- 291 N. Mahmood, C. Z. Zhang, J. Jiang, F. Liu and Y. L. Hou, *Chem-Eur. J.*, 2013, **19**, 5183-5190.
- 292 J. Choi, J. Jin, I. G. Jung, J. M. Kim, H. J. Kim and S. U. Son, *Chem. Commun.*, 2011, **47**, 5241-5243.
- 293 N. Li, H. W. Song, H. Cui and C. X. Wang, *Nano Energy*, 2014, **3**, 102-112.
- 294 S. Han, D. Q. Wu, S. Li, F. Zhang and X. L. Feng, *Adv. Mater.*, 2014, **26**, 849-864.
- 295 W. Wei, S. B. Yang, H. X. Zhou, I. Lieberwirth, X. L. Feng and K. Mullen, *Adv. Mater.*, 2013, **25**, 2909-2914.
- 296 Y. H. Hwang, E. G. Bae, K. S. Sohn, S. Shim, X. Song, M. S. Lah and M. Pyo, *J. Power Sources*, 2013, **240**, 683-690.
- 297 C. D. Wang, Y. Li, Y. S. Chui, Q. H. Wu, X. F. Chen and W. J. Zhang, *Nanoscale*, 2013, **5**, 10599-10604.
- 298 Z. P. Chen, W. C. Ren, L. B. Gao, B. L. Liu, S. F. Pei and H. M. Cheng, *Nat. Mater.*, 2011, **10**, 424-428.
- 299 X. Cao, Y. Shi, W. Shi, G. Lu, X. Huang, Q. Yan, Q. Zhang and H. Zhang, *Small*, 2011, **7**, 3163-3168.
- 300 J. S. Luo, J. L. Liu, Z. Y. Zeng, C. F. Ng, L. J. Ma, H. Zhang, J. Y. Lin, Z. X. Shen and H. J. Fan, *Nano Lett.*, 2013, **13**, 6136-6143.
- 301 N. Li, Z. P. Chen, W. C. Ren, F. Li and H. M. Cheng, *Proc. Natl. Acad. Sci. U. S. A.*, 2012, **109**, 17360-17365.

- 302 H. Y. Sun, Y. G. Liu, Y. L. Yu, M. Ahmad, D. Nan and J. Zhu, *Electrochim. Acta*, 2014, **118**, 1-9.
- 303 H. Gwon, H. S. Kim, K. U. Lee, D. H. Seo, Y. C. Park, Y. S. Lee, B. T. Ahn and K. Kang, *Energy Environ. Sci.*, 2011, **4**, 1277-1283.
- 304 C. Yuan, L. Yang, L. Hou, J. Li, Y. Sun, X. Zhang, L. Shen, X. Lu, S. Xiong and X. W. Lou, *Adv. Funct. Mater.*, 2012, **22**, 2560-2566.
- 305 T. Hu, X. Sun, H. Sun, M. Yu, F. Lu, C. Liu and J. Lian, *Carbon*, 2013, **51**, 322-326.
- 306 A. P. Yu, H. W. Park, A. Davies, D. C. Higgins, Z. W. Chen and X. C. Xiao, *J. Phys. Chem. Lett.*, 2011, **2**, 1855-1860.
- 307 R. H. Wang, C. H. Xu, J. Sun, Y. Q. Liu, L. Gao and C. C. Lin, *Nanoscale*, 2013, **5**, 6960-6967.
- 308 Z. Bo, W. Zhu, W. Ma, Z. Wen, X. Shuai, J. Chen, J. Yan, Z. Wang, K. Cen and X. Feng, *Adv. Mater.*, 2013, **25**, 5799-5806.
- 309 N. Li, H. Song, H. Cui and C. X. Wang, *Electrochim. Acta*, 2014, **130**, 670-678.
- 310 Z. Bo, K. Yu, G. Lu, S. Cui, S. Mao and J. Chen, *Energy Environ. Sci.*, 2011, **4**, 2525-2528.
- 311 N. Li, H. W. Song, H. Cui, G. W. Yang and C. X. Wang, *J. Mater. Chem. A*, 2014, **2**, 2526-2537.
- 312 N. Li, S. X. Jin, Q. Y. Liao, H. Cu and C. X. Wang, *Nano Energy*, 2014, **5**, 105-115.
- 313 W. P. Kang, Y. B. Tang, W. Y. Li, Z. P. Li, X. Yang, J. Xu and C. S. Lee, *Nanoscale*, 2014, **6**, 6551-6556.
- 314 D. Z. Chen, H. Y. Quan, J. F. Liang and L. Guo, *Nanoscale*, 2013, **5**, 9684-9689.
- 315 Y. Shi, J. Z. Wang, S. L. Chou, D. Wexler, H. J. Li, K. Ozawa, H. K. Liu and Y. P. Wu, *Nano Lett.*, 2013, **13**, 4715-4720.
- 316 D. Y. Chen, W. X. Chen, L. Ma, G. Ji, K. Chang and J. Y. Lee, *Mater. Today*, 2014, **17**, 184-193.
- 317 C. D. Wang, Y. S. Chui, R. G. Ma, T. L. Wong, J. G. Ren, Q. H. Wu, X. F. Chen and W. J. Zhang, *J. Mater. Chem. A*, 2013, **1**, 10092-10098.
- 318 S. B. Yang, X. L. Feng and K. Mullen, *Adv. Mater.*, 2011, **23**, 3575-3579.
- 319 R. Thomas and G. M. Rao, *Electrochim. Acta*, 2014, **125**, 380-385.
- 320 X. F. Zhou, W. J. Liu, X. Y. Yu, Y. J. Liu, Y. P. Fang, S. Klankowski, Y. Q. Yang, J. E. Brown and J. Li, *ACS Appl. Mater. Inter.*, 2014, **6**, 7434-7443.
- 321 W. B. Yue, S. S. Tao, J. M. Fu, Z. Q. Gao and Y. Ren, *Carbon*, 2013, **65**, 97-104.
- 322 C. F. Zhang, X. Peng, Z. P. Guo, C. B. Cai, Z. X. Chen, D. Wexler, S. Li and H. K. Liu, *Carbon*, 2012, **50**, 1897-1903.
- 323 W. Fan, W. Gao, C. Zhang, W. W. Tjiu, J. S. Pan and T. X. Liu, *J. Mater. Chem.*, 2012, **22**, 25108-25115.
- 324 F. Yao, F. Güneş, H. Q. Ta, S. M. Lee, S. J. Chae, K. Y. Sheem, C. S. Cojocaru, S. S. Xie and Y. H. Lee, *J. Am. Chem. Soc.*, 2012, **134**, 8646-8654.
- 325 F. Y. Su, Y. B. He, B. H. Li, X. C. Chen, C. H. You, W. Wei, W. Lv, Q. H. Yang and F. Y. Kang, *Nano Energy*, 2012, **1**, 429-439.
- 326 W. Wei, W. Lv, M.-B. Wu, F.-Y. Su, Y.-B. He, B. Li, F. Kang and Q.-H. Yang, *Carbon*, 2013, **57**, 530-533.
- 327 S. Q. Chen, Y. Wang, H. Ahn and G. X. Wang, *J. Power Sources*, 2012, **216**, 22-27.
- 328 D. N. Wang, X. F. Li, J. L. Yang, J. J. Wang, D. S. Geng, R. Y. Li, M. Cai, T. K. Sham and X. L. Sun, *Phys. Chem. Chem. Phys.*, 2013, **15**, 3535-3542.
- 329 X. Zhou, J. Bao, Z. Dai and Y.-G. Guo, *The J. Phys. Chem. C*, 2013, **117**, 25367-25373.
- 330 F. R. Beck, R. Epur, D. H. Hong, A. Manivannan and P. N. Kumta, *Electrochim. Acta*, 2014, **127**, 299-306.
- 331 M. Zhang, D. Lei, Z. F. Du, X. M. Yin, L. B. Chen, Q. H. Li, Y. G. Wang and T. H. Wang, *J. Mater. Chem.*, 2011, **21**, 1673-1676.
- 332 P. C. Lian, X. F. Zhu, S. Z. Liang, Z. Li, W. S. Yang and H. H. Wang, *Electrochim. Acta*, 2011, **56**, 4532-4539.
- 333 X. Y. Wang, X. F. Zhou, K. Yao, J. G. Zhang and Z. P. Liu, *Carbon*, 2011, **49**, 133-139.
- 334 Z. H. Wen, S. M. Cui, H. J. Kim, S. Mao, K. H. Yu, G. H. Lu, H. H. Pu, O. Mao and J. H. Chen, *J. Mater. Chem.*, 2012, **22**, 3300-3306.
- 335 X. S. Zhou, L. J. Wan and Y. G. Guo, *Adv. Mater.*, 2013, **25**, 2152-2157.
- 336 L. Wang, D. Wang, Z. H. Dong, F. X. Zhang and J. Jin, *Nano Lett.*, 2013, **13**, 1711-1716.
- 337 S. J. R. Prabakar, Y. H. Hwang, E. G. Bae, S. Shim, D. Kim, M. S. Lah, K. S. Sohn and M. Pyo, *Adv. Mater.*, 2013, **25**, 3307-3312.
- 338 B. B. Chen, H. Qian, J. H. Xu, L. L. Qin, Q. H. Wu, M. S. Zheng and Q. F. Dong, *J. Mater. Chem. A*, 2014, **2**, 9345-9352.

- 339 P. C. Lian, X. F. Zhu, H. F. Xiang, Z. Li, W. S. Yang and H. H. Wang, *Electrochim. Acta*, 2010, **56**, 834-840.
- 340 S. K. Behera, *Chem. Commun.*, 2011, **47**, 10371-10373.
- 341 X. Wang, W. Tian, D. Q. Liu, C. Y. Zhi, Y. Bando and D. Golberg, *Nano Energy*, 2013, **2**, 257-267.
- 342 P. C. Lian, S. Z. Liang, X. F. Zhu, W. S. Yang and H. H. Wang, *Electrochim. Acta*, 2011, **58**, 81-88.
- 343 M. Zhang, D. N. Lei, X. Z. Yu, L. B. Chen, Q. H. Li, Y. G. Wang, T. H. Wang and G. Z. Cao, *J. Mater. Chem.*, 2012, **22**, 23091-23097.
- 10 344 P. Chen, Y. Su, H. Liu and Y. Wang, *Acs Appl. Mater. Inter.*, 2013, **5**, 12073-12082.
- 345 X. H. Cao, Y. M. Shi, W. H. Shi, X. H. Rui, Q. Y. Yan, J. Kong and H. Zhang, *Small*, 2013, **9**, 3433-3438.
- 346 S. L. Chou, J. Z. Wang, M. Choucair, H. K. Liu, J. A. Stride and S. X. Dou, *Electrochem. Commun.*, 2010, **12**, 303-306.
- 15 347 L. W. Ji, H. H. Zheng, A. Ismach, Z. K. Tan, S. D. Xun, E. Lin, V. Battaglia, V. Srinivasan and Y. G. Zhang, *Nano Energy*, 2012, **1**, 164-171.
- 348 Y. J. Du, G. N. Zhu, K. Wang, Y. G. Wang, C. X. Wang and Y. Y. Xia, *Electrochim. Commun.*, 2013, **36**, 107-110.
- 349 H. Li, C. X. Lu and B. P. Zhang, *Electrochim. Acta*, 2014, **120**, 96-101.
- 20 350 C. F. Guo, D. L. Wang, T. F. Liu, J. S. Zhu and X. S. Lang, *J. Mater. Chem. A*, 2014, **2**, 3521-3527.
- 351 R. Z. Hu, W. Sun, Y. L. Chen, M. Q. Zeng and M. Zhu, *J. Mater. Chem. A*, 2014, **2**, 9118-9125.
- 352 D. Li, K. H. Seng, D. Q. Shi, Z. X. Chen, H. K. Liu and Z. P. Guo, *J. Mater. Chem. A*, 2013, **1**, 14115-14121.
- 25 353 Y. Ding, Y. Jiang, F. Xu, J. Yin, H. Ren, Q. Zhuo, Z. Long and P. Zhang, *Electrochim. Commun.*, 2010, **12**, 10-13.
- 354 X. F. Zhou, F. Wang, Y. M. Zhu and Z. P. Liu, *J. Mater. Chem.*, 2011, **21**, 3353-3358.
- 355 J. L. Yang, J. J. Wang, D. N. Wang, X. F. Li, D. S. Geng, G. X. Liang, M. Gauthier, R. Y. Li and X. L. Sun, *J. Power Sources*, 2012, **208**, 340-344.
- 30 356 J. Mun, H. W. Ha and W. Choi, *J. Power Sources*, 2014, **251**, 386-392.
- 357 B. Wang, K. F. Li, D. W. Su, H. J. Ahn and G. X. Wang, *Chem. Asian J.*, 2012, **7**, 1637-1643.
- 358 S. Evers and L. F. Nazar, *Chem. Commun.*, 2012, **48**, 1233-1235.
- 359 N. W. Li, M. B. Zheng, H. L. Lu, Z. B. Hu, C. F. Shen, X. F. Chang, G. B. Ji, J. M. Cao and Y. Shi, *Chem. Commun.*, 2012, **48**, 4106-4108.
- 35 360 J. Q. Huang, X. F. Liu, Q. Zhang, C. M. Chen, M. Q. Zhao, S. M. Zhang, W. C. Zhu, W. Z. Qian and F. Wei, *Nano Energy*, 2013, **2**, 314-321.
- 361 B. Ding, C. Z. Yuan, L. F. Shen, G. Y. Xu, P. Nie, Q. X. Lai and X. G. Zhang, *J. Mater. Chem. A*, 2013, **1**, 1096-1101.
- 362 L. Wang, D. Wang, F. X. Zhang and J. Jin, *Nano Lett.*, 2013, **13**, 4206-4211.
- 40 363 W. D. Zhou, H. Chen, Y. C. Yu, D. L. Wang, Z. M. Cui, F. J. DiSalvo and H. D. Abruna, *ACS Nano*, 2013, **7**, 8801-8808.
- 364 R. J. Chen, T. Zhao, J. Lu, F. Wu, L. Li, J. Z. Chen, G. Q. Tan, Y. S. Ye and K. Amine, *Nano Lett.*, 2013, **13**, 4642-4649.
- 365 X. Yang, L. Zhang, F. Zhang, Y. Huang and Y. Chen, *ACS Nano*, 2014.
- 45 366 G. M. Zhou, S. F. Pei, L. Li, D. W. Wang, S. G. Wang, K. Huang, L. C. Yin, F. Li and H. M. Cheng, *Adv. Mater.*, 2014, **26**, 625-631.
- 367 H. D. Liu, P. Gao, J. H. Fang and G. Yang, *Chem. Commun.*, 2011, **47**, 9110-9112.
- 368 C. V. Rao, A. L. M. Reddy, Y. Ishikawa and P. M. Ajayan, *Acs Appl. Mater. Inter.*, 2011, **3**, 2966-2972.

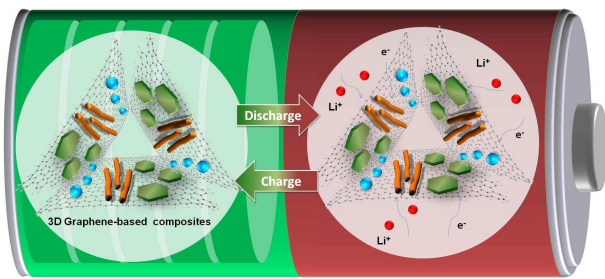
50

# Design and construction of three dimensional graphene-based composites for lithium ion battery applications

Bin Luo, Linjie Zhi\*

DOI: 10.1039/b000000x [DO NOT ALTER/DELETE THIS TEXT]

Graphical Abstract:



This review summarizes the current progress on the synthesis of three-dimensional graphene-based composites and their applications for lithium ion battery.

# Design and construction of three dimensional graphene-based composites for lithium ion battery applications

Bin Luo, Linjie Zhi\*

<sup>5</sup> DOI: 10.1039/b000000x [DO NOT ALTER/DELETE THIS TEXT]

**Broader context:** Lithium-ion batteries (LIBs) are becoming more and more attractive for the ever-enlarging markets of portable electronic products, communication facilities, and electric vehicles. Huge demand has motivated <sup>10</sup> scientific and technological efforts dedicated to developing LIBs with superior performances, such as higher energy density, higher power density, and longer cycle life. To achieve these characters, many materials have been investigated as electrode materials for LIBs. Rationally designed three dimensional graphene-based composites (3DGCs) have emerged as promising candidates for electrode <sup>15</sup> materials in lithium ion batteries. In this review, recent progress on 3DGCs encompassing their preparation and application in lithium ion batteries is summarized, shedding light particularly on the view point of structural and interfacial engineering which have demonstrated to play critically important role for the development of high performance electrode systems. Their advantages <sup>20</sup> and disadvantages are compared and summarized based on the results published in the literatures, new trends of graphene-based electrode materials for high-performance LIBs are discussed as well.